3-8-2021

Carbon Storage of Restored Mangrove Forests in Biscayne Bay, Florida

Daniel Chomin-Virden
5730290@fiu.edu

FLORIDA INTERNATIONAL UNIVERSITY

Miami, Florida

CARBON STORAGE OF RESTORED MANGROVE FORESTS IN BISCAYNE BAY, FLORIDA

A thesis submitted in partial fulfillment of

the requirements for the degree of

MASTER OF SCIENCE

in

BIOLOGY

by

Daniel Chomin-Virden

2021

To: Dean Michael R. Heithaus
College of Arts, Sciences, and Education

This thesis, written by Daniel Chomin-Virden, and entitled Carbon Storage of Restored Mangrove Forests in Biscayne Bay, Florida, having been approved in respect to style and intellectual content, is referred to you for judgment.

We have read this thesis and recommend that it be approved.

Jennifer H. Richards

James W. Fourqurean

Michael S. Ross

Tiffany G. Troxler, Major Professor

Date of Defense: March 8, 2021

The thesis of Daniel Chomin-Virden is approved.

Dean Michael R. Heithaus
College of Arts, Sciences and Education

Andrés G. Gil
Vice President for Research and Economic Development
and Dean of the University Graduate School

Florida International University, 2021

DEDICATION

To Emma. To love that frees.

ACKNOWLEDGMENTS

I wish to thank the countless friends and colleagues that have made this work possible. Thank you Shelby, Nick, Ben, and Vivi for helping me find my footing at the beginning of all this. Thank you Tanja, Ariel, Talin, and Christina for listening to my woes and comforting me with yours. Thank you to Team Mangrove: Juliana, Nasreen, and Jackie for inspiring me to study mangroves; Heather and Krystyna, for inspiring me to see this through to the end.

Thank you to all my amazing volunteers: Chrisean, Jennyfer, Miguel, Shantel, Alex, and everyone who lent me their time in this pursuit. Thank you to the members of the Wetland Ecosystems Lab; all of you have been tremendously patient and accommodating through the continuing work. Dr. Edward Castaneda, your guidance was essential to my understanding of the history of mangrove ecology. The Seagrass Lab was also a tremendous help in conceptualizing and implementing my work. Special thanks to Dr. Donny Smoak at the University of South Florida for his generosity with his time and with his work; without his support the carbon accumulation analysis would not have been possible.

Thank you to Miami-Dade County and the State of Florida for the use of your parks for my research. Thank you in particular to Josh Mahoney, for orienting me to the sites and helping me make the most of them. Thank you to Gary Milano for your pioneering work in restoring mangroves in Miami-Dade County, and for sharing with me the history of your work. Thank you to Guy Forchion and the Historic Virginia Key Beach Park Trust for access and use of your park. Thank you to Elizabeth Golden and Chelsie Young for your assistance in accessing the state parks for my research.

Thank you to the Department of Biology for your moral and material support; your dedication to your students is always felt. Thank you to my committee; to Dr. Jim Fourqurean and Dr. Mike Ross for your time and consideration, to Dr. Richards for helping me to know what I can do, and to my major professor, Dr. Troxler, for pushing me to dream bigger than what I can see.

Thank you to my family, for supporting me without fail throughout my academic career, and for not asking me too often when I expect to graduate. Emma, thank you for your patience and support, and for reminding me that taking care of myself is a valuable use of my time.

ABSTRACT OF THE THESIS

CARBON STORAGE OF RESTORED MANGROVE FORESTS IN BISCAYNE BAY, FLORIDA

by

Daniel Chomin-Virden

Florida International University, 2021

Miami, Florida

Professor Tiffany G. Troxler, Major Professor

Space-for-time substitution was used to evaluate the rate of carbon storage in three carbon pools (aboveground, belowground, and soil organic carbon) across four restored mangrove forests in Biscayne Bay, Florida, USA. The restored forests ranged in age from 8 to 20 years. Diameter at breast height was used to estimate aboveground biomass. Belowground biomass and soil carbon were determined using 15 cm soil cores. Time to equivalence was calculated for the sites by reference to geographically proximate natural mangrove forests. Time to equivalence in aboveground and belowground biomass were 50.4 and 13.6 years, respectively. Soil organic carbon and total carbon stock did not display a linear trend over time. The study did not show the anticipated recovery within 20 years, but the results varied widely by carbon pool. The study suggests mangrove restorations seeking to match the carbon storage from natural forests should expect a longer time to recovery.

TABLE OF CONTENTS

LIST OF TABLES

LIST OF FIGURES

CHAPTER I. Carbon Mitigation Potential of Natural and Restored Mangrove Ecosystems: A Key Part of the Portfolio Toward Global Negative Carbon Dioxide Emissions

1. Introduction

The release of carbon dioxide (CO_2) into the atmosphere is the largest anthropogenic contributor to climate change (IPCC 2014). Carbon dioxide leaves the atmosphere when it diffuses directly into the ocean or is removed from the air by photosynthesizing organisms such as plants. Intertidal or subtidal vegetation such as mangroves, marshes, or seagrasses that store significant amounts of carbon are referred to as “blue carbon ecosystems” (Crooks et al. 2019); of these three major blue carbon ecosystems, the greatest carbon (C) per unit area is stored in mangrove forests (Lovelock et al. 2019). Mangrove forests are intertidal ecosystems with woody plants and are globally distributed across tropical and subtropical latitudes (Mukherjee et al. 2014). Mangroves survive in a variety of salinities and tidal ranges, producing substantial physiological variation both within and among their approximately 70 species (Alongi 2014) and supporting substantial coastal productivity (Twilley et al. 2017). Blue carbon is one of several “negative emissions technologies” (NETs), which are approaches to draw down atmospheric CO_2 levels (NASEM 2019). To avoid the most significant impacts of climate change, NETs would need to be deployed to sequester 10 Gt per year over the next 10 years (NASEM 2019). While the capacity for emissions reduction by blue carbon is among the lowest NETs when scaled to US and global capacities, restoration and creation of blue carbon ecosystems offer additional benefits, or ecosystem services, beyond C mitigation and cost significantly less than alternative NETs (NASEM 2019).

Mangrove forests provide ecosystem services that can be categorized into three major groups: provisioning, regulating, and supporting services (Millennium Ecosystem Assessment 2005, Vegh et al. 2019). The provisioning services are the resources that can be directly harvested from mangrove forests, which have historically included timber and charcoal, fish and shells (López-Angarita et al. 2016). The regulating services are those that are mediated through ecosystem processes. For example, mangroves provide coastal protection by reducing wind and wave energy by up to 66% (McIvor et al. 2012), filter nutrients from wastewater (Robertson and Phillips 1995), and promote sedimentation by trapping organic and sedimentary material (Horstman et al. 2014). The supporting services mangroves provide enhanced conditions for other organisms. Mangroves provide habitat for reptiles, mammals, birds, fish, and invertebrates (Nagelkerken et al. 2008). For fish in particular, mangroves serve as nurseries, providing shelter, sources of food, and reduced predation for fish that support recreational and commercial fisheries (Barbier et al. 2011, Whitfield 2017). The blue carbon service provided by mangroves can be considered both a supporting service, for building soil and trapping nutrients to be used by other organisms, and a regulating service, for its concurrent effect capturing CO_2 from the atmosphere.

Resulting from their location along tropical and subtropical shorelines, mangroves have faced significant development pressure; approximately 1/3 of global mangrove forest area was destroyed in the years between 1950 and 2000 (Lovelock et al. 2019). The specific causes and degree of loss vary by region, with the greatest loss in recent years occurring in southeast Asia, where aquaculture and logging are the greatest proximate threats (Thomas et al. 2017).

The blue carbon storage of mangroves and other coastal ecosystems has prompted global and national efforts to quantify the C mitigation benefits provided through their conservation, creation, and restoration (NASEM 2019). However, because the carbon mitigation benefit of created and restored forests can not necessarily be approximated from natural forests, additional research is needed to determine the carbon mitigation benefit that planted mangrove forests can provide. This review highlights the carbon stored by natural and restored mangrove forests in each of three major C pools: aboveground biomass, belowground biomass, and soil C. For each pool, the variation among global mangrove forests is explored, along with the rate of C storage at different ages of the restoration process.

2. Carbon Storage in Natural Mangrove Forests

Carbon sequestration refers to the process through which plants and other photosynthesizing organisms capture CO_2 from the atmosphere and convert it to biomass (Windham-Myers et al. 2019). Average C stored by tropical terrestrial forests range from an average of 140 Mg C/ha (95% confidence interval: 133-148 Mg C/ha) in South America to 197 Mg C/ha (95% confidence interval: 180-215 Mg C/ha) in Asia (Sullivan et al. 2017), while mangrove forests in their most productive region average 1023 ± 88 Mg C/ha, with some forests reaching over 2200 Mg C/ha (Donato et al. 2011). Mangroves are able to sequester large stocks of soil C through morphological traits such as extensive aboveground root structures which trap leaves and sediment in place, contributing to deposition of decomposed organic matter as peat (Lugo 1997, Gillis et al. 2016). Dead roots are also a significant component of mangrove peat (Alongi 2012).

Mangrove peat-building enables the land-building service mangroves provide, accumulating meters of peat over the course of centuries or millennia (e.g., Ezcurra et al. 2016).

Natural mangrove forests can serve as a useful reference for whether a mangrove forest restoration has been successful, and often rates of natural mangrove forest C storage and accumulation are used to estimate the C benefit of created and restored mangrove forests. However, the C storage benefit of mangroves is highly sensitive to environmental conditions, and restoration efforts must be balanced against competing social priorities and opportunity costs (Romañach et al. 2018) which may resist the creation of the ideal growing conditions found in the natural forests for which many studies have been completed. To make meaningful comparisons between natural and restored mangrove forests, it is important to understand the environmental factors that influence C storage and the methods of measuring the C that is stored.

3. Environmental Influences on C Storage

A. Nutrient Availability

The quantity of C stored by mangrove forests varies by species and according to environmental conditions including nutrient availability and hydrology. Castañeda et al. (2013) found mangroves in the Florida coastal Everglades varied in productivity and forest structure (characteristics which influence C storage) according to soil phosphorus, soil sulfide concentration, and the frequency and duration of inundation, with 52% of the variation attributed to phosphorus availability. Phosphorus limitation can cause mangroves to take on stunted growth forms, limiting aboveground biomass and slowing belowground C storage (Feller 1995). For example, phosphorus limitation in the Florida Everglades is a contributing factor in creating "dwarf" mangrove scrub forests, mangrove forests in which the average tree height is under 3 meters (Rivera-Monroy et al. 2011).

B. Hydrology

The influence of hydrology on mangrove forest structure is one of the longest-studied aspects of mangrove ecology, tracing back to Watson's hydrological classification of the mangrove forests of Malaysia (Watson 1928)**.** Watson observed that mangrove forests could be grouped into distinct forest types according to the tidal cycle, elevation, and frequency of inundation. These factors are aggregated into five numbered "classes," ranging from Class 1 sites, which are too inundated for mangrove survival, to Class 5 sites, which are inundated too rarely for most mangroves to outcompete non-mangrove species, with Class 3 sites at the peak frequency to allow diverse mangrove species to flourish. Subsequent researchers have modified Watson's classification system to simplify and generalize its applicability. For example, Van Loon (2016) highlights a system that reduces the variables to elevation and duration of inundation, utilizing both total daily minutes of inundation and total length of time per inundation to account for diverse tidal regimes without needing to specify the number of inundations per day (Van Loon et al. 2016).

Rovai et al. (2018) used hydrological and geomorphological factors such as riverine and tidal influences on salinity and sediment supply to classify forests into distinct coastal ecological settings (CES). They then developed a model for estimating carbon storage in mangrove forests according to CES. Thirty-six (36) mangrove forest sites from previous studies, representing a broad range in geography and mangrove species, were each classified into one of nine CES. Sites were then compared to identify the primary drivers of inter-group variation in mangrove soil organic carbon (SOC), finding tidal amplitude and minimum temperature to be the most important factors distinguishing soil C storage in mangroves in different CES. Rovai et al. (2018) attributed the tidal influence to the ability of tides to supplement nutrient levels in mangrove forests, aerate soils, and regulate organic matter (OM) decomposition. The effect of temperature was attributed to its effect on OM decomposition and root growth. The authors compared the SOC estimated by their model against the SOC estimation in Jardine and Saakimäki's 2014 model attributing regional variation among mangroves to a climatic gradient. Rovai et al. (2018) found the climatic model underestimated mangrove SOC in carbonate settings by 44%, and overestimated SOC in deltaic settings by 86%. Combining the CES model with high-resolution mangrove forest cover maps, three of the researchers from Rovai et al. (2018) estimated the global mangrove SOC at 2.3 Pg C (Twilley et al. 2018). The model developed by Rovai et al. (2018) demonstrated the importance of hydrology in mangrove forest C storage.

4. Measurement of C Pools

The methods used to calculate the C stored in mangrove forests have a significant influence on our knowledge of the C stored in the forests. Stored C is measured using components of the total C "stock." Mangrove forest C stock is the sum of the C stored in four different pools: aboveground live biomass, aboveground dead biomass, belowground biomass, and soil C (Howard et al. 2014). The aboveground live biomass is the mass of all aboveground components of the living trees in the forest: the wood, the leaves, and the aboveground roots. The biomass is converted to mass of C by either direct elemental analysis of dried, ground biomass or by the use of a C conversion factor, a ratio of C per unit mass determined for a particular mangrove species by a previous direct measurement. The aboveground dead biomass is the total of those same components (wood, leaves, and roots) for any fallen trees and any broken off limbs within the study area. The aboveground dead biomass is measured separately because the C stored in each tree decreases as the tree decomposes and loses biomass. The belowground biomass is the mass of all the subterranean roots of the trees, and the soil C is the C stored in the soil itself, enriched by decomposing leaves, branches, and roots. Soil C measurements include C stored *in situ* by the mangroves on site ("autochthonous" C), and C captured elsewhere and transported to the mangrove forest by water, wind, or living organisms ("allochthonous" C). The C stock is measured by measuring the C in each of these pools in vegetation plots or transects, then converting those measurements into C stored per unit area. If the stock of the entire forest is sought, the C per unit area is multiplied across the area of the forest for a total C stock. Mangrove forest C storage can be compared by their storage per unit area, usually in megagrams C per hectare (MgC/ha) (Howard et al. 2014).

A. Aboveground Live Biomass

Direct measurement of aboveground live biomass (AGB) is completed by cutting down trees, drying the samples, and weighing all the constituent parts of the tree (Howard et al. 2014). The direct method is inherently highly destructive; therefore, researchers have developed alternative means of measuring aboveground biomass. One common non-destructive way to measure mangrove biomass is through allometric measurements, where a correlation is found in a previous direct measurement between the trees' biomass and an easily-measured attribute of the trees such as height or diameter at breast height (DBH) (Fromard et al. 1998, Smith and Whelan 2006, Howard et al. 2014). Allometric equations are species- and region-specific, so the equation used must be one that was developed in a location as similar to the area of interest as possible, both in proximity and environmental conditions (Komiyama et al. 2008). The specificity of allometric equations is the result of mangroves' sensitivities to a wide range of environmental factors that are controlled for within the region where the equation is developed (Adame et al. 2017). In a review of over 50 mangrove C stock assessments, Komiyama et al. (2008) found aboveground live biomass in mangrove forests to range from 7.9 Mg/ha to 460 Mg/ha.

B. Aboveground Dead Biomass

Non-destructive measurements of aboveground dead biomass C also use the DBH of the trees to estimate the biomass with an allometric equation; however, the biomass estimate is modified according to each tree's "decay status" (Howard et al. 2014). For standing dead trees that are mostly whole but defoliated, the allometric equation for the live aboveground biomass would be used, then the leaf volume would be subtracted according to a leaf-specific biomass equation. For dead trees in a further state of decay, the percent of the volume lost from branches can be estimated, using a 10-20% estimate for an intact stem with only some branches missing. For severely decayed trunks missing significant segments from their stems, the volume can be estimated using the equation for the volume of a cone, then the biomass calculated using a reference wood density for the species. The C content of the dead wood biomass can be estimated at 50% (Kauffman and Donato 2012). One study of C stock in a mangrove forest in Chiapas, Mexico, found an average of 29.4 MgC/ha stored in aboveground dead biomass (referred to as "downed wood"), which was approximately 13% of the mean C stored in aboveground live biomass (Adame et al. 2015). A study of a mangrove forest in the Zambezi River Delta in Mozambique found dead standing tree biomass to make up 4% of the total aboveground biomass (Trettin et al. 2016).

C. Belowground Live Biomass

Direct measurement of belowground biomass can be made in several ways. Like aboveground live biomass, belowground live biomass can be directly measured through highly destructive methods, the excavation and removal of entire mangrove root systems (Adame et al. 2017). A less destructive sampling method is to subsample mangrove root biomass within narrow soil cores; however, this methodology necessarily excludes large root biomass, as the coring apparatus may not able to cut through large roots, so sampling locations are generally selected that avoid the large roots (Adame et al. 2017). Non-destructive allometric methods using DBH, like those for above-ground biomass, have been used for belowground biomass; however, far fewer species-specific allometric equations have been developed for estimating belowground live C than for live aboveground biomass (Howard et al. 2014, Adame et al. 2017). To accommodate for the difficulty of producing numerous species-specific equations for belowground biomass, Komiyama et al. developed a general equation that can be used to calculate the belowground biomass of mangroves that do not have a species-specific equation (Komiyama et al. 2005). Allometric equations for belowground biomass are constrained by a considerable amount of uncertainty; in a meta-analysis comparing published direct measurement samples of belowground root biomass to Komiyama's general equation and several species-specific allometric equations, Adame et al. (2017) found Komiyama's general equation to produce values 40 ± 12% higher than the values reported from narrow core measurement of belowground biomass. Howard et al. (2014) recommend using a C content of 0.39 for belowground live biomass.

D. Soil C

Soil C is measured by taking a sediment core from within the mangrove forest, then measuring the soil mass, bulk density, and carbon content directly (Howard et al. 2014). The soil coring method used is decided by the soil mineral content and the soil depth. Mangrove forests with low sediment input and high retention of organic material such as leaves and roots develop darker, "organic" soils. Organic carbon (OC) is the C stored through retention of organic material. Mangrove forests with high sediment input and lower retention of organic material develop lighter-colored "inorganic" soils containing high concentrations of calcium carbonate. Inorganic carbon (IC) is the C stored by other processes such as marl production or deposition of calcareous marine invertebrates. Total Carbon (TC) is the sum of both OC and IC. When studying the soil C of highly organic soils, the OC is roughly equivalent to the TC. When studying soils with both OC and IC, the OC can be found by subtracting the inorganic carbon (IC) from the TC (OC = TC – IC). Mangrove forests can develop layers of organic soil over 3 meters deep (Howard et al. 2014); however, examination of deeper cores can be prohibitively labor-intensive, therefore most analyses limit their scope to the top meter or less, following Kauffman and Donato's recommendation (Kauffman and Donato 2012). Rovai et al. (2018) estimated average soil OC stocks in the top meter of soils to range from 250 to over 500 MgC/ha across environmental settings.

5. Carbon Storage in Restored Mangrove Forests

The C stored by mangrove restorations is typically studied in reference to a natural forest in close geographic proximity and having similar hydrogeological conditions (Salmo et al. 2013). Comparison between restored and natural forests is often made in reference to the "time to equivalence," the amount of time in years after restoration required before the value of interest is equivalent in magnitude to the value in the natural reference sites (Osland et al. 2012). Time to equivalence is estimated by evaluating the value of C stored in sites of different ages using a method called "space-for-time" substitution. Space-for-time substitution evaluates similar sites of different ages since restoration as "snapshots" across a common growth trajectory for the restored mangrove system, enabling efficient study of long-term ecological trends.

One example of the space-for-time substitution approach is Osland et al.'s (2012) study comparing natural and restored mangrove forests in Tampa Bay, FL. The forests in Osland et al.'s study contained a mix of red, white, and black mangroves (*Rhizophora mangle*, *Laguncularia racemosa*, and *Avicennia germinans*, respectively). A 20-year chronosequence was established using nine mangrove restorations, which were compared to geographically proximate reference sites of natural mangrove forest. The study found soil TC reached equivalence with natural mangroves in 20 years. The study did not report the C stored in aboveground biomass but estimated a time to equivalence of 25 years for adult tree diameter (a common indicator used to estimate total aboveground biomass through allometry). All the natural reference sites in the study had organic soils, with a mean natural reference value for soil TC of 144.2 ± 16.4 g C/kg.

DelVecchia et al. (2014) did not use space-for-time substitution, instead comparing two restorations of similar age (10 years) and an afforested site (age 20 years) to natural mangrove sites of unknown age. The study of natural and restored red mangrove (*Rhizophora mangle*) forests in Muisne, Ecuador, found equivalent soil C stored in natural and restored forests, with 1-m-deep soil cores containing an average soil C of 0.055 ± 0.002 g/cm^3 in natural mangrove forests and an average soil C of 0.058 ± 0.002 g/cm^3 in restored forests (DelVecchia et al. 2014). The authors found the soil C to be 411.6 ± 27.9 MgC/ha in the restored sites and 365.3 ± 23.8 MgC/ha in the natural sites. While the difference between these values is not statistically significant, the authors noted this finding of greater soil C in the restored sites contradicts that of Osland et al. (2012), which did not report C stock but clearly showed 10-year-old restorations bearing transitional C values trending toward the natural reference. DelVecchia et al. (2014) suggest the prior land use at their study site (shrimp farms) may have played a role in enriching C storage at the Muisne mangrove restorations.

Salmo et al. (2013), studying *Rhizophora mucronata* stands in the Philippines, estimated that *Rhizophora mucronata* stands in the Philippines would reach equivalent DBH, AGB, and soil OM in approximately 25 years. In addition to comparing raw values of these features, the authors also studied each site three to five times over the course of 2 years, enabling them to identify the change in each measurement over time. Frequent measures as in Salmo et al. (2013) provide robust data, but are extremely resource intensive, preventing wide application.

6. Economic Mangrove Restoration for C Storage

One key factor in promoting carbon storage through mangrove restoration is the need for a market that accounts for the C storage benefit that mangroves provide. A market can contextualize the ecological benefit from mangrove restoration so that investments in mangrove restoration can be balanced against alternative C management strategies (Barbier 2013, Locatelli et al. 2014). The VM0033 Tidal Wetland and Seagrass Restoration Methodology is a system created to align wetland restoration, including mangrove restoration, with the Verified Carbon Standard, the largest global carbon standard (Needelman et al. 2019). The VM0033 methodology lays out a standardized way to account for the C and other greenhouse gases (GHGs) stored by wetland restoration projects by estimating the existing GHG stock, projecting the GHG storage rate under "business as usual" conditions, and estimating the GHG storage rate predicted for a restoration project (Emmer et al. 2015). By comparing the business-as-usual scenario to the restoration scenario, the methodology provides an estimate of reduction in CO_2 equivalents (a standard unit for carbon markets that accounts for both CO_2 and other greenhouse gases), which can be converted to credits for sale in a carbon market. Mangroves are well-suited to marketed restoration because they produce forests with significant aboveground C storage in the short- to medium-term (for immediate, quantifiable gains) in addition to their long-term soil C storage potential (Locatelli et al.

2014). Under the methodology, projects may estimate the expected mangrove soil C storage rate by using a published rate from a similar location or by using a default value of 1.46 t C/ha/year (1.32 MgC/ha/year) (Needelman et al. 2019).

At present, there is not a global C market where mangrove forest C credits can be sold; however, national and international markets are available (Vegh et al. 2019). The carbon standards have established agreements with registries to facilitate the sale of credits from approved projects for voluntary C credit sale; proposed mangrove projects could apply for inclusion on one of these registries (Lee et al. 2018). The Mikoko Pamoja mangrove restoration project in Gazi Bay, Kenya, is one of the first mangrove restoration projects to be financed through the sale of carbon credits (Wylie et al. 2016). Through an agreement with Edinburgh organization Plan Vivo, credits representing one metric ton of C are sold for between 6.50 USD and 10.00 USD.

Regulations requiring compensation for destroyed forests play a part in slowing the loss of mangrove forests. In the United States, mangroves are protected at the federal level by Section 404 of the Clean Water Act, which regulates dredging or filling of waters of the United States, including coastal wetlands such as mangrove forests (Hough and Robertson 2009). Section 404 requires that impacts to wetlands be minimized, and unavoidable impacts be mitigated. In Florida, USA, where most mangroves in the United States are located (Romañach et al. 2018), mangroves are protected by the Mangrove Trimming and Preservation Act of 1996 (Florida Statutes § 403.9321), which requires any trimming of existing mangroves be performed by a licensed professional and establishes morphological benchmarks for the level of protection afforded to mangroves. Both federal and state protection in Florida are focused on the preservation of and compensation for mangroves that remain; neither framework provides an incentive for increasing mangrove restoration beyond the current extent.

7. Carbon Storage and Other Ecosystem Services

Under certain circumstances, mangrove C storage can compete with the other ecosystem services that mangroves provide. For example, when mangroves are used to treat unfiltered wastewater, it can lead to increases in emissions of N_2O and CH_4, counteracting the climate benefits of mangrove C storage with these more potent greenhouse gases (Konnerup et al. 2014). A study of riverine mangroves along the Danshuei River in northern Taiwan found the mangroves decreased river velocity, increasing flooding; this resulted in a need to clear a portion of the mangroves and sacrifice their C storage potential in order to reduce river flooding (Shih et al. 2015). The same study noted that as mangroves spread into mud flats, this necessarily reduces the habitat available to fauna that live in or migrate through the mud flats. When quantifying the benefits of mangrove forest restoration, the secondary impacts of the restoration must also be accounted for.

Even when mangroves are not restored specifically to store C, C storage will result as an ancillary benefit. Mangrove restoration in Florida is often motivated by the other ecosystem services mangroves provide, including their role as fish nurseries and their ability to stabilize shorelines (Milano 1999). Still, using the C benefit as a lens for selection of restoration sites has been shown to be a reliable strategy for securing water purification and coastal stabilization, as the quality of these services are closely linked (Adame et al. 2014).

8. Conclusion

Mangrove forest restoration has the potential to contribute to global C storage strategies. Mangrove forests provide both rapid C storage in aboveground biomass and long-term, continual C sequestration through development of thick layers of mangrove peat. Preservation of existing mangrove forests is also essential considering the large C stock stored within peat layers accumulated over hundreds or thousands of years. Additional research is needed to better understand how the rate of mangrove C storage varies within different ecological contexts. This research will inform region-specific climate planning and support international cooperation by providing insight into where and how to allocate mitigation funding.

9. List of References

Adame, M. F., S. Cherian, R. Reef, and B. Stewart-Koster. 2017. Mangrove root biomass and the uncertainty of belowground carbon estimations. Forest Ecology and Management 403:52–60.

Adame, M. F., V. Hermoso, K. Perhans, C. E. Lovelock, and J. a. Herrera-Silveira. 2014. Selecting cost-effective areas for restoration of ecosystem services. Conservation Biology 29:493–502.

Adame, M. F., N. S. Santini, C. Tovilla, A. Vázquez-Lule, L. Castro, and M. Guevara. 2015. Carbon stocks and soil sequestration rates of tropical riverine wetlands. Biogeosciences 12:3805–3818.

Alongi, D. M. 2012. Carbon sequestration in mangrove forests. Carbon Management 3:313–322.

Alongi, D. M. 2014. Carbon cycling and storage in mangrove forests. Annual Review of Marine Science 6:195–219.

Barbier, E. 2013. Valuing Ecosystem Services for Coastal Wetland Protection and Restoration: Progress and Challenges. Resources 2:213–230.

Barbier, E. B., S. D. Hacker, C. Kennedy, E. W. Koch, A. C. Stier, and B. R. Silliman. 2011. The value of estuarine and coastal ecosystem services. Ecological Monographs 81:169–193.

Crooks, S., L. Windham-Myers, and T. G. Troxler. 2019. Defining Blue Carbon. Pages 1–8 *in* L. Windham-Myers, S. Crooks, and T. G. Troxler, editors. A Blue Carbon Primer: The State of Coastal Wetland Carbon Science, Practice, and Policy. CRC Press, Boca Raton, FL.

DelVecchia, A. G., J. F. Bruno, L. Benninger, M. Alperin, O. Banerjee, and J. de Dios Morales. 2014. Organic carbon inventories in natural and restored Ecuadorian mangrove forests. PeerJ 2:e388.

Donato, D. C., J. B. Kauffman, D. Murdiyarso, S. Kurnianto, M. Stidham, and M. Kanninen. 2011. Mangroves among the most carbon-rich forests in the tropics. Nature Geoscience 4:293–297.

Emmer, I. M., B. A. Needelman, S. Emmett-Mattox, S. Crooks, J. P. Megonigal, D. Myers, M. P. J. Oreska, K. J. McGlathery, D. Shoch, V. C. S. Methodology, and S. Scope. 2015. Methodology for Tidal Wetland and Seagrass Restoration:1–115.

Ezcurra, P., E. Ezcurra, P. P. Garcillán, M. T. Costa, and O. Aburto-Oropeza. 2016. Coastal landforms and accumulation of mangrove peat increase carbon sequestration and storage. Proceedings of the National Academy of Sciences of the United States of America 113:4404–4409.

Feller, I. C. 1995. Effects of Nutrient Enrichment on Growth and Herbivory of Dwarf Red Mangrove (Rhizophora Mangle). Ecological Monographs 65:477–505.

Fromard, F., H. Puig, L. Cadamuro, G. Marty, J. L. Betoulle, and E. Mougin. 1998. Structure, above-ground biomass and dynamics of mangrove ecosystems: new data from French Guiana. Oecologia 115:39–53.

Gillis, L. G., M. Zimmer, and T. J. Bouma. 2016. Mangrove leaf transportation: Do mimic Avicennia and Rhizophora roots retain or donate leaves? Marine Ecology Progress Series 551:107–115.

Horstman, E. M., C. M. Dohmen-Janssen, P. M. F. Narra, N. J. F. van den Berg, M. Siemerink, and S. J. M. H. Hulscher. 2014. Wave attenuation in mangroves: A quantitative approach to field observations. Coastal Engineering 94:47–62.

Hough, P., and M. Robertson. 2009. Mitigation under Section 404 of the Clean Water Act: Where it comes from, what it means. Wetlands Ecology and Management 17:15–33.

Howard, J., S. Hoyt, K. Isensee, E. Pidgeon, and M. Telszewski. 2014. Coastal Blue Carbon: Methods for assessing carbon stocks and emissions factors in mangroves, tidal salt marshes, and seagrass meadows. Arlington, Virginia.

IPCC. 2014. Climate Change 2014: Synthesis Report. Geneva, Swirzerland.

Kauffman, J. B., and D. C. Donato. 2012. Protocols for the measurement, monitoring and reporting of structure, biomass and carbon stocks in mangrove forests. Page Center for International Forestry.

Komiyama, A., J. E. Ong, and S. Poungparn. 2008. Allometry, biomass, and productivity of mangrove forests: A review. Aquatic Botany 89:128–137.

Komiyama, A., S. Poungparn, and S. Kato. 2005. Common allometric equations for estimating the tree weight of mangroves. Journal of Tropical Ecology 21:471–477.

Konnerup, D., J. M. Betancourt-Portela, C. Villamil, and J. P. Parra. 2014. Nitrous oxide and methane emissions from the restored mangrove ecosystem of the Ciénaga Grande de Santa Marta, Colombia. Estuarine, Coastal and Shelf Science 140:43–51.

Lee, D. H., D. hwan Kim, and S. il Kim. 2018. Characteristics of forest carbon credit transactions in the voluntary carbon market. Climate Policy 18:235–245.

Locatelli, T., T. Binet, J. G. Kairo, L. King, S. Madden, G. Patenaude, C. Upton, and M. Huxham. 2014. Turning the Tide: How Blue Carbon and Payments for Ecosystem Services (PES) Might Help Save Mangrove Forests. Ambio:981–995.

Van Loon, A. F., B. Te Brake, M. H. J. Van Huijgevoort, and R. Dijksma. 2016. Hydrological classification, a practical tool for mangrove restoration. PLoS ONE 11:1–26.

López-Angarita, J., C. M. Roberts, A. Tilley, J. P. Hawkins, and R. G. Cooke. 2016. Mangroves and people: Lessons from a history of use and abuse in four Latin American countries. Forest Ecology and Management 368:151–162.

Lovelock, C. E., D. A. Friess, J. B. Kauffman, and J. W. Fourqurean. 2019. Human Impacts on Blue Carbon Ecosystems. Pages 17–24 *in* L. Windham-Myers, S. Crooks, and T. G. Troxler, editors. A Blue Carbon Primer: The State of Coastal Wetland Carbon Science, Practice and Policy. CRC Press, Boca Raton, FL.

Lugo, A. E. 1997. Old-growth mangrove forests in the United States. Conservation Biology 11:11–20.

McIvor, A., I. Möller, T. Spencer, and M. Spalding. 2012. Reduction of Wind and Swell Waves by Mangroves. Page Natural Coastal Protection Series.

Milano, G. R. 1999. Restoration of coastal wetlands in southeastern florida. Wetland Journal 11:15–24.

Millennium Ecosystem Assessment. 2005. Ecosystems and human well-being: Wetlands and water synthesis. Washington, DC.

Mukherjee, N., W. J. Sutherland, M. N. I. Khan, U. Berger, N. Schmitz, F. Dahdouh-Guebas, and N. Koedam. 2014. Using expert knowledge and modeling to define mangrove composition, functioning, and threats and estimate time frame for recovery. Ecology and Evolution 4:2247–2262.

Nagelkerken, I., S. J. M. Blaber, S. Bouillon, P. Green, M. Haywood, L. G. Kirton, J. O. Meynecke, J. Pawlik, H. M. Penrose, A. Sasekumar, and P. J. Somerfield. 2008. The habitat function of mangroves for terrestrial and marine fauna: A review. Aquatic Botany 89:155–185.

NASEM. 2019. Negative Emissions Technologies and Reliable Sequestration. Page Negative Emissions Technologies and Reliable Sequestration. National Academies Press.

Needelman, B. A., I. M. Emmer, M. P. J. Oreska, and J. P. A. Megonigal. 2019. Blue Carbon Accounting for Carbon Markets. Page *in* L. Windham-Myers, S. Crooks, and T. G. Troxler, editors. Blue Carbon Primer: The State of Coastal Wetland Carbon Science, Practice and Policy. CRC Press, Boca Raton, FL.

Osland, M. J., A. C. Spivak, J. A. Nestlerode, J. M. Lessmann, A. E. Almario, P. T. Heitmuller, M. J. Russell, K. W. Krauss, F. Alvarez, D. D. Dantin, J. E. Harvey, A. S. From, N. Cormier, and C. L. Stagg. 2012. Ecosystem Development After Mangrove Wetland Creation: Plant-Soil Change Across a 20-Year Chronosequence. Ecosystems 15:848–866.

Rivera-Monroy, V. H., R. R. Twilley, S. E. Davis, D. L. Childers, M. Simard, R. Chambers, R. Jaffe, J. N. Boyer, D. T. Rudnick, K. Zhang, E. Castañeda-Moya, S. M. L. Ewe, R. M. Price, C. Coronado-Molina, M. Ross, T. J. Smith, B. Michot, E. Meselhe, W. Nuttle, T. G. Troxler, and G. B. Noe. 2011. The Role of the Everglades Mangrove Ecotone Region (EMER) in Regulating Nutrient Cycling and Wetland Productivity in South Florida. Critical Reviews in Environmental Science and Technology 41:633–669.

Robertson, A. I., and M. J. Phillips. 1995. Mangroves as filters of shrimp pond effluent : predictions and biogeochemical research needs. Hydrobiologia 295:311–321.

Romañach, S. S., D. L. DeAngelis, H. L. Koh, Y. Li, S. Y. Teh, R. S. Raja Barizan, and L. Zhai. 2018. Conservation and restoration of mangroves: Global status, perspectives, and prognosis. Ocean and Coastal Management 154:72–82.

Rovai, A. S., R. R. Twilley, E. Castañeda-Moya, P. Riul, M. Cifuentes-Jara, M. Manrow-Villalobos, P. A. Horta, J. C. Simonassi, A. L. Fonseca, and P. R. Pagliosa. 2018. Global controls on carbon storage in mangrove soils. Nature Climate Change 8:534–538.

Salmo, S. G., C. Lovelock, and N. C. Duke. 2013. Vegetation and soil characteristics as indicators of restoration trajectories in restored mangroves. Hydrobiologia 720:1–18.

Shih, S.-S., H.-L. Hsieh, P.-H. Chen, C.-P. Chen, and H.-J. Lin. 2015. Tradeoffs between reducing flood risks and storing carbon stocks in mangroves. Ocean & Coastal Management 105:116–126.

Smith, T. J., and K. R. T. Whelan. 2006. Development of allometric relations for three mangrove species in South Florida for use in the Greater Everglades Ecosystem restoration. Wetlands Ecology and Management 14:409–419.

Sullivan, M. J. P., J. Talbot, S. L. Lewis, O. L. Phillips, L. Qie, S. K. Begne, J. Chave, A. Cuni-Sanchez, W. Hubau, G. Lopez-Gonzalez, L. Miles, A. Monteagudo-Mendoza, B. Sonké, T. Sunderland, H. Ter Steege, L. J. T. White, K. Affum-Baffoe, S. I. Aiba, E. C. De Almeida, E. A. De Oliveira, P. Alvarez-Loayza, E. Á. Dávila, A. Andrade, L. E. O. C. Aragão, P. Ashton, G. A. Aymard, T. R. Baker, M. Balinga, L. F. Banin, C. Baraloto, J. F. Bastin, N. Berry, J. Bogaert, D. Bonal, F. Bongers, R. Brienen, J. L. C. Camargo, C. Cerón, V. C. Moscoso, E. Chezeaux, C. J. Clark, Á. C. Pacheco, J. A. Comiskey, F. C. Valverde, E. N. H. Coronado, G. Dargie, S. J. Davies, C. De Canniere, M. N. Djuikouo, J. L. Doucet, T. L. Erwin, J. S. Espejo, C. E. N. Ewango, S. Fauset, T. R. Feldpausch, R. Herrera, M. Gilpin, E. Gloor, J. S. Hall, D. J. Harris, T. B. Hart, K. Kartawinata, L. K. Kho, K. Kitayama, S. G. W. Laurance, W. F. Laurance, M. E. Leal, T. Lovejoy, J. C. Lovett, F. M. Lukasu, J. R. Makana, Y. Malhi, L. Maracahipes, B. S. Marimon, B. H. M. Junior, A. R. Marshall, P. S. Morandi, J. T. Mukendi, J. Mukinzi, R. Nilus, P. N. Vargas, N. C. P. Camacho, G. Pardo, M. Peña-Claros, P. Pétronelli, G. C. Pickavance, A. D. Poulsen, J. R. Poulsen, R. B. Primack, H. Priyadi, C. A. Quesada, J. Reitsma, M. Réjou-Méchain, Z. Restrepo, E. Rutishauser, K. A. Salim, R. P. Salomão, I. Samsoedin, D. Sheil, R. Sierra, M. Silveira, J. W. F. Slik, L. Steel, H. Taedoumg, S. Tan, J. W. Terborgh, S. C. Thomas, M. Toledo, P. M. Umunay, L. V. Gamarra, I. C. G. Vieira, V. A. Vos, O. Wang, S. Willcock, and L. Zemagho. 2017. Diversity and carbon storage across the tropical forest biome. Scientific Reports 7:1–12.

Thomas, N., R. Lucas, P. Bunting, A. Hardy, A. Rosenqvist, and M. Simard. 2017. Distribution and drivers of global mangrove forest change, 1996-2010. PLoS ONE 12:1996–2010.

Trettin, C. C., C. E. Stringer, and S. J. Zarnoch. 2016. Composition, biomass and structure of mangroves within the Zambezi River Delta. Wetlands Ecology and Management 24:173–186.

Twilley, R. R., E. Castañeda-Moya, V. H. Rivera-Monroy, and A. Rovai. 2017. Productivity and Carbon Dynamics in Mangrove Wetlands. Pages 113–162 *in* V. H. Rivera-Monroy, S. Y. Lee, E. Kristensen, and R. R. Twilley, editors. Mangrove Ecosystems: A Global Biogeographic Perspective. Springer International Publishing, Cham, Switzerland.

Twilley, R. R., A. S. Rovai, and P. Riul. 2018. Coastal morphology explains global blue carbon distributions. Frontiers in Ecology and the Environment 16:503–508.

Vegh, T., L. Pendleton, B. Murray, T. Troxler, K. Zhang, E. Castañeda-Moya, G. Guannel, and A. Sutton-Grier. 2019. Ecosystem Services and Economic Valuation: Co-Benefits of Coastal Wetlands. Pages 250–266 *in* L. Windham-Myers, S. Crooks, and T. G. Troxler, editors. A Blue Carbon Primer: The State of Coastal Wetland Carbon Science, Practice and Policy. CRC Press, Boca Raton, FL.

Watson, J. G. 1928. Mangrove Forests of the Malay Peninsula. Fraser & Neave.

Whitfield, A. K. 2017. The role of seagrass meadows, mangrove forests, salt marshes and reed beds as nursery areas and food sources for fishes in estuaries. Reviews in Fish Biology and Fisheries 27:75–110.

Windham-Myers, L., S. Crooks, and T. G. Troxler. 2019. A Blue Carbon Primer: The State of Coastal Wetland Carbon Science, Practice and Policy. Page (L. Windham-Myers, S. Crooks, and T. G. Troxler, Eds.). CRC Press, Boca Raton, FL.

Wylie, L., A. E. Sutton-Grier, and A. Moore. 2016. Keys to successful blue carbon projects: Lessons learned from global case studies. Marine Policy 65:76–84.

CHAPTER II. Carbon Storage in Restored Mangrove Forests in Biscayne Bay, Florida

1. Introduction

Mangrove forests are salt-tolerant, coastal, hardwood ecosystems found in tropical latitudes around the world (Mukherjee et al. 2014). Mangroves have faced significant threats from agriculture, aquaculture, and urban development, with over 35% of all mangrove forests having been destroyed since 1980 (Romañach et al. 2018). Mangroves provide a variety of ecosystem services, including habitat for a wide range of terrestrial and aquatic wildlife (Nagelkerken et al. 2008), protection from wind and wave energy (Zhang et al. 2012, Das and Crépin 2013), and sequestration of carbon (Donato et al. 2011). When mangrove forests are destroyed for development, they are no longer able to provide these services, as the ecological structure and productivity fundamental to these services is degraded or lost.

The carbon (C) sequestered by mangroves, along with coastal marshes and seagrasses, is known as "blue carbon" (Crooks et al. 2019). Blue carbon ecosystems are significant, as they store significantly more C than terrestrial ecosystems covering the same areal extent; mangrove ecosystems store more than twice as much C in tons per hectare than boreal, temperate, or tropical forests (Alongi 2012). Mangrove C is overwhelmingly stored within mangrove soil, built up over hundreds and sometimes thousands of years as C is converted into leaf and root matter then trapped and broken down into mangrove peat. Conversion of mangrove forests for development results in the release of that C as CO_2 (Lovelock et al. 2019). One way to counteract these effects is by restoring lost ecosystems so they can resume sequestering C.

Miami, Florida, USA, is a highly urbanized coastal city where the effects of development claimed 82% of the mangrove forest by 1976 (Harlem 1979). To restore coastal wetlands, including mangrove forests, Miami-Dade County Department of Environmental Resource Management (DERM) developed the Coastal Wetland Restoration Program (CWRP) (Milano 1999a). The CWRP was also interested in the ecosystem services provided by restored wetlands, especially habitat for native species and shoreline stabilization (Milano 1999a, 2000). In 2010, Miami-Dade County developed its Climate Action Plan, which included habitat restoration as one of its environmental goals, suggesting C offset programs as a possible funding stream (Miami-Dade County 2010).

To determine the amount of C credits available from a proposed ecosystem restoration project, it is necessary to know the amount of C anticipated to be stored by the project and how it compares to a "business-as-usual" scenario without the restoration project (Emmer et al. 2015). The type and strength of ecosystem services provided by coastal wetlands are dependent on the specific qualities of the ecosystems providing them (Folke et al. 2004), particularly in mangrove forests, which are made up of a few species with highly plastic growth forms that reflect hydrology and nutrient profile (Feller et al. 2010). Storage of C in natural mangrove forests is well studied (Donato et al. 2011, Alongi 2014, Ribeiro et al. 2019), but because of mangroves' variable growth rates and forms, there is a need to study C storage in restored mangrove forests, particularly in urban environments, to understand the potential C benefit of restored mangrove forests.

The present study aims to identify how the C storage service varies in time and space in restored mangrove forests on a narrow urban coastline relative to mature, natural mangrove forests in a similar hydrogeologic setting. Previous research found that for restored mangrove forests in Tampa, Florida, soil organic matter (SOM) in the top 10 cm of soil reached equivalency to proximate natural mangrove forests after 20 years (Osland et al. 2012). Accordingly, I expected the C stored in restored mangrove forests around Biscayne Bay to reach equivalence with local natural reference sites after 20 years. To measure the change in stored C over time, I used a "space-for-time" approach in which contemporary sites representing differing lengths of time since establishment were used in the absence of long-term ecological data. The space-for-time approach has been used previously to evaluate mangrove restorations in the Philippines (Salmo et al. 2013, 2014) and Tampa Bay, FL, USA (Osland et al. 2012, Krauss et al. 2017). The present study is the first attempt to apply the space-for-time approach to mangrove restoration sites in Biscayne Bay in Miami, Florida.

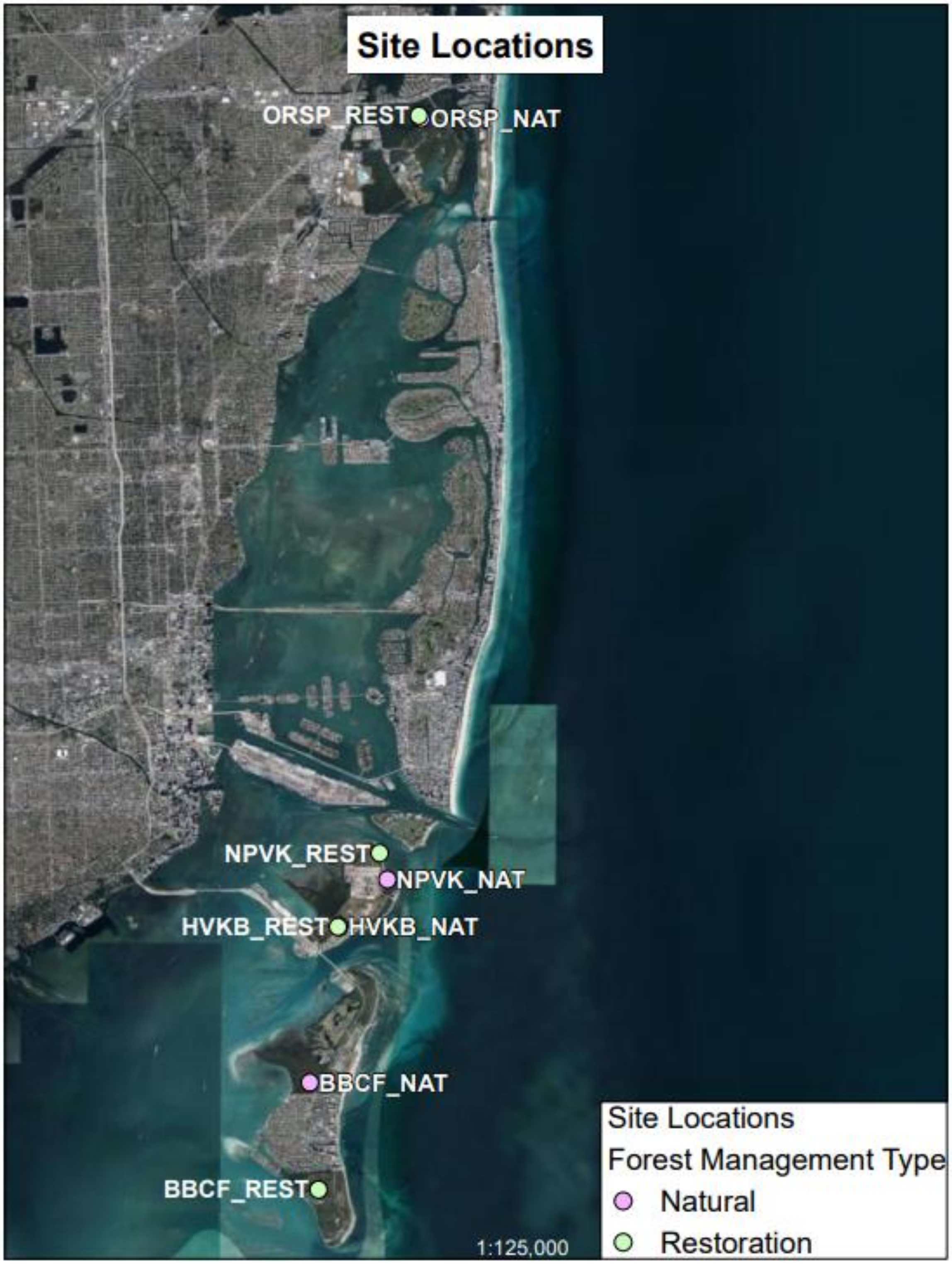

Figure 1: Site Locations. Location of each natural and restored mangrove forest studied in Biscayne Bay.

Figure 2: Plot Locations. Close-up of the four mangrove restorations. Sites: Bill Baggs Cape Florida State Park (BBCF), North Point Virginia Key (NPVK), Oleta River State Park (ORSP), Historic Virginia Key Beach Park (HVKB).

2. Methods

A. Study Sites

Four restored mangrove forests around Biscayne Bay were selected with the assistance of Miami-Dade DERM (Figure 1). The sites were located at Bill Baggs Cape Florida State Park (BBCF), at the north point of Virginia Key (NPVK), at the Historic Virginia Key Beach Park (HVKB), and at Oleta River State Park (ORSP) (Figure 2). The restoration sites selected were fringe mangrove forests restored by Miami-Dade County's DERM CWRP 20, 19, 10, and 8 years, respectively, prior to the beginning of the study. The sites were restored by adjusting the elevation using a backhoe to scrape coastal areas to elevations appropriate for mangrove establishment: 1.0'-1.2' NGVD for red mangrove (*Rhizophora mangle*) areas; 1.25'-1.5' for black mangrove (*Avicennia germinans*) areas; and 1.5'-2.0' for white mangrove (*Laguncularia racemosa*) areas (Milano 1999a). The restoration sites were planted by both contractors and volunteers with one-year-old red mangrove saplings (Milano 1999a). Saplings were planted on a 3' center, a density of approximately 1.2 plants/m^2 (Milano 1999a). White and black mangroves were typically not planted because of their abundance in surrounding areas, providing ample recruits without individual planting. Instead, areas targeting black or white mangroves would be leveled to the appropriate grade and allowed to recruit naturally (Milano 1999a). Specific attributes of each site are described below (Table 1). Natural reference sites were selected by identifying mature mangrove forests in close geographic proximity to each restoration site. Exact plot locations for each forest management type ("restoration" and "natural reference" or "natural") were selected by identifying areas with relatively uniform canopy height accessible on foot. An onsite mature mangrove forest was selected as the natural reference for sites where such forests were available (HVKB, ORSP). For the other two sites (BBCF, NPVK), the nearest available mature forest along the same coast was selected as the natural reference site.

Table 1: Site Conditions. Four restorations in Miami-Dade County, FL, USA were selected for study. Mature mangrove forests in close geographic proximity to each restoration were selected to serve as natural reference sites.

Restored Sites

Site Name	Code	Age of Restoration (Year Completed)	Latitude (Decimal Degrees)	Longitude (Decimal Degrees)	Restoration Size (Acres)	Notes on Site Condition
Bill Baggs Cape Florida State Park	BBCF_REST	20 (1998)	25.67835	-80.16125	65	Site historically filled for recreational use; following Hurricane Andrew site scraped to buried, pre-fill organic soil
North Point, Virginia Key	NPVK_REST	19 (1999)	25.75506	-80.14731	3.75	Site located atop extension of coast from Government Cut dredge spoil
Historic Virginia Key Beach Park	HVKB_REST	10 (2008)	25.73826	-80.15681	35	Site located along a tidal channel at 900 m from the shoreline, resulting in restricted tidal flushing
Oleta River State Park	ORSP_REST	8 (2010)	25.92317	-80.13836	22.2	Site located on the Oleta River at the site of a former marina, scraped to buried, pre-fill organic soil

Natural Sites

Site Name	Code	Proximity to Restoration (m)	Latitude (Decimal Degrees)	Longitude (Decimal Degrees)	Notes on Site Condition
Calusa Park	BBCF_NAT	2710	25.70276	-80.16322	Site located 600 m inland along mosquito ditch
Lamar Lake	NPVK_NAT	690	25.74904	-80.14552	Site located near wastewater treatment plant, primary tidal exchange through a culvert
Historic Virginia Key Beach Park	HVKB_NAT	25	25.73825	-80.15656	Site located directly across tidal creek from HVKB Restoration; Natural site includes some invasive exotics
Oleta River State Park	ORSP_NAT	90	25.92252	-80.13779	Site located directly across Oleta River from ORSP Restoration

Bill Baggs Cape Florida State Park is located on the southern point of Key Biscayne (Figure 2, BBCF_REST_1-3). Aerial imagery from 1925 shows the west coast of the key with mangrove cover, but in the 1950's the site was filled with dredged sediment from Biscayne Bay to elevate the grade for development (Milano 1999b). In 1992, Hurricane Andrew destroyed a large area of invasive vegetation, with significant cover of Australian pine (*Casuarina equisetifolia*), creating an opportunity for the county to restore 65 acres of red mangrove forest on the west coast property (Liddell 2003). The restoration included a series of pools and channels to facilitate hydrologic flow (Milano 1999b). This restoration was completed in phases, and the phase containing the site used in this study was completed in 1998 (Liddell 2003). For a natural reference site, I selected Calusa Park, a Miami-Dade County park on the west side of Key Biscayne and part of Crandon Park, as it is the geographically closest mature mangrove forest on the west coast of Key Biscayne (Figure 2, BBCF_NAT_1-3).

The first of the two restoration projects on Virginia Key that were studied was located at the northern point of Virginia Key (Figure 2, NPVK_REST_1-3). This area is built out from the historical coast, originally extended with dredge spoil from the widening of Government Cut (Harlem 1979). The shape of the restoration is a narrow "lasso" shape, with a narrow channel encircling a raised forest area. This restoration was completed in 1999 (Liddell 2003). The natural reference for this site is the mature mangrove forest on the east side of Virginia Key, adjacent to Lamar Lake, selected for both its proximity and ease of access (Figure 2, NPVK_NAT_1-3).

The second restoration on Virginia Key is located at the Historic Virginia Key Beach Park (Figure 2, HVKB_REST_1-3), a city-owned park on the eastern coast of Virginia Key. The restoration area is located adjacent to the park on land owned by Miami-Dade County, which had suffered extensive invasion by Australian pine ("Virginia Key Master Plan" 2010). The non-native vegetation was removed and replaced with a range of native ecosystems including forests of red and black mangroves; the black mangrove forests were left to recruit naturally, and the red mangroves finished planting in 2008 (Gary Milano, personal communication).The HVKB site includes a long mosquito ditching channel through the park, providing limited tidal flow to different sections of the restored area along its bounds ("Virginia Key Master Plan" 2010). The location selected for the present study was roughly 900 m from the shore along this channel, at a point across the channel from the mature forest that was selected to serve as its natural reference site (Figure 2, HVKB_NAT_1-3).

The final restoration site is a 22.2-acre triangular restoration with its long edge along the Oleta River in Oleta River State Park (Figure 2, ORSP_REST_1-3). Records from as late as 1925 recognized much of this area as freshwater marl prairie, but following significant dredging in what came to be known as the Interama property, as well as an increased nutrient load from rapid urbanization upriver, mangroves colonized the prairie and began to prosper (Teas 1974, Harlem 1979). In the 1960's, the newly grown mangrove forest was dredged and filled to create a marina along the Oleta River (Florida Department of Environmental Protection 2008). The property became part of the state park in 1985, and the former marina was selected for restoration in the 2000s

(Florida Department of Environmental Protection 2008). Like the restoration at BBCF, the site includes pools and channels; restoration was completed in 2010 (Gary Milano, personal communication). The natural reference forest for this site is the mature mangrove forest directly across the river from the restoration (Figure 2, ORSP_NAT_1-3), which has grown uninterrupted since the initial expansion into the prairie (Harlem 1979).

In each of the 4 restoration and natural sites, three 10 x 10 m vegetation plots were established. The plots were located 20 m apart and 5 m away from the nearest water channel or river, measured from the mean extent of red mangrove prop roots into the water.

B. Hydrology

Water levels were measured using a combination of water level gauges and manual depth-to-water (DTW) measurements. In each plot, three 5.08 cm (2 in) diameter PVC wells approximately 1 m in length were installed 50 cm deep into the soil, approximately 2.5 m apart along a straight line extending from the center of the water-ward side of the plot, enabling measurements 2.5 m, 5.0 m, and 7.5 m from the edge of the plot. In one well at each restoration site, an Onset HOBO pressure gauge was installed to collect water level data at half-hour intervals, while all other wells at the restoration sites and all natural site wells were ungauged. At ORSP and HVKB, an additional HOBO sensor was placed in the well above the expected maximum water level to correct measurements for variation in barometric pressure. Sites were then visited bimonthly to manually record DTW and download gauge measurements. An average offset was calculated from the mean difference between the manual water level measurements at each ungauged well and the gauge in the restoration plot. The offset was used to approximate water levels at each ungauged well from the water levels collected by the gauge between manual water level measurements. These adjusted water levels were used to determine hydroperiod for each plot, characterized as “flood frequency” in floods per year and “flood duration” in hours flooded per year (October 2017 – October 2018). A site was considered flooded any time the water level was at or above the soil surface (water level ≥ 0 m). Flood frequency was standardized by calculating floods per day (the total number of independent submersion events observed at a site divided by the total number of days for which data was collected at that site) and multiplying by 365 days to yield floods per year (greatest loss at site NPVK, missing data from May 6th to August 3rd). Similarly, flood duration was standardized by calculating hours flooded per day (the total number of hours the site was submerged over the course of the study divided by the total number of days for which data was recorded) and multiplying by 365 days to yield hours flooded per year.

C. Forest Structure

In each plot, every red, black, and white mangrove with a diameter at breast height (DBH) of 2.5 cm or larger was marked with an aluminum tag. Tagged trees were measured for DBH and height. The DBH was measured using diameter tape at 1.3 m or above the highest prop root (whichever was higher), and tree height was measured with a telescopic rod. Density was measured as tagged mangrove tree count per unit area, and basal area for each tagged tree was calculated from its diameter. Trees less than 2.5 cm DBH were not measured as part of the study.

D. Carbon Storage in Aboveground Biomass

My study examined carbon storage in three carbon pools: aboveground live biomass, belowground biomass, and soil carbon. Aboveground live biomass was estimated using allometric equations developed by Smith and Whelan (2006) relating mangrove DBH to aboveground dry biomass in kg. These equations were developed in South Florida, so they are expected to approximate the aboveground biomass of Biscayne Bay's mangroves more closely than equations developed in other regions. Carbon content was then estimated using a 0.44 ratio of mass carbon to aboveground biomass (Ewe et al. 2006).

*Table 2: Allometric Equations. Allometric equations for calculating aboveground biomass (AGB) from diameter at breast height (DBH) along with the diameter range at which the equations are most accurate. Equations are provided for the three mangrove species found in South Florida, black mangrove (*Avicennia germinans*), white mangrove (*Laguncularia racemosa*), and red mangrove (*Rhizophora mangle*). The equations were developed by Smith & Whelan (2006) using direct measurement of South Florida mangroves.*

Equation Number	**Species**	**Equation**	**Diameter range (cm)**
Equation 1	*Avicennia germinans*	AGB $=0.403*(DBH)^{1.934}$	2.5-21.5
Equation 2	*Laguncularia racemosa*	AGB $=0.362*(DBH)^{1.930}$	2.5-18.0
Equation 3	*Rhizophora mangle*	AGB $=0.722*(DBH)^{1.731}$	2.5-20.0

E. Carbon Storage in Belowground Biomass and Soil

In each plot, one 15 cm soil core was collected. Sediment accumulation rates for mangrove forests vary widely, but previous research found South Florida mangroves to accumulate sediment within a range of 0.6 – 7.2 mm/year (Sasmito et al. 2016). Because the oldest restoration in the study was 20 years old, I determined 15 cm cores to be sufficient for comparing the restored forests to natural forests. Cores were collected using a 15.24 cm (6-inch) diameter PVC suction-corer. Cores were capped and transported out of the field in the PVC corer, which was placed in ice and transported back to the lab. Using a custom-made core extruder (manufactured by Nolan's Machine Shop, Lafayette, LA, USA, according to specifications sent by Dr. Edward Castañeda, Research Associate Professor at Florida International University), soil cores were then pressed out of the PVC corer and cut into 1 cm segments. Half of each segment was frozen and archived, while the other half-section (hereafter "sample") was frozen until being processed for analysis. Samples were thawed for 24 hours, then weighed. Samples were dried at 60°C until constant weight, then finely ground with mortar and pestle and stored in 20 ml glass scintillation vials. Total carbon (TC) and total nitrogen (TN) for each sample was found using a FlashEA 1112 elemental analyzer (Thermo Scientific) (Howard et al. 2014). Inorganic C (IC) content for each sample was then determined by ashing a subsample of the dried soil sample at 500°C for 4 hours and running the ashed subsample through the elemental analyzer. The mass of organic C (OC) in grams was determined by multiplying the mass of TC by 100 minus the percent IC, and the percent OC of the subsection was determined by dividing the mass of OC by the subsection dry mass. The soil OC measured in this way was used as the soil C pool.

Roots and rocks larger than 2 mm in diameter ("large roots and rocks") were removed during grinding and weighed; these weights were subtracted from the dry mass of the soil. Large root volumes and rock volumes were measured using water displacement and subtracted from the sample's total volume before calculating bulk density. Bulk density was measured as the dry mass without the large roots and rocks divided by the sample's total volume without the large roots and rocks, measured in grams per cubic centimeter. The belowground biomass was determined from the dry mass of the large roots (including live and dead roots) removed during the grinding process. Belowground biomass C was determined by multiplying the belowground biomass by the 0.44 C conversion rate.

F. Soil Carbon Accumulation Rate

The rate of soil C accumulation was estimated using ^{210}Pb, half-life 22.3 years, using the methods described in Smoak et al. (2013) and Breithaupt et al. (2014). Due to the costly and time-consuming nature of ^{210}Pb sampling, 4 cores were selected to be sampled, one restored and one natural plot from the oldest restoration (BBCF) and from the youngest restoration (ORSP). From each dried, ground, 1 cm subsection of these 4 cores, a 4 mL subsample was set aside in a 7 mL scintillation vial and sent to the University of South Florida for processing. After samples were packed into gamma counting tubes, an intrinsic germanium well detector coupled to a multi-channel analyzer was used to measure gamma activity. ^{210}Pb activity was measured at the 46.5 keV peak, and background ^{226}Ra was measured with its surrogate, ^{214}Pb, at 351.9 keV. While ^{137}Cs is sometimes used for additional validation of ^{210}Pb analyses, highly organic mangrove soils can cause ^{137}Cs to leach out of the soil, compromising its utility as an independent verification of ^{210}Pb dates (Breithaupt et al. 2014). For this reason, ^{137}Cs validation was not used. Instead, ^{210}Pb response trends were compared to redox-sensitive ^{238}U (measured via a ^{234}Th proxy) to gain additional insight into the soil profiles.

In the restored sites, the ^{210}Pb activity-versus-depth profile was expected to show a steady decline in ^{210}Pb activity with a sudden break that would indicate the boundary between sediment accumulated since restoration and the pre-restoration sediment below the excavation depth. The percent OC and soil bulk density profiles were also compared to this breaking point to confirm the depth of the breaking point. Soil C accumulation rate in grams C per meter squared per year ($gC/m^2/yr$) was then determined as the sum of the soil C in all segments above the breaking point divided by the depth. Mass accumulation was calculated similarly, by summing the mass in grams per meter squared (g/m^2) above the breaking point and dividing it by the time since restoration in years. Total sediment accretion was determined by dividing the depth of the break in cm by the time since restoration in years and multiplying by 10 for units of millimeters per year (mm/yr).

Natural sites were expected to have deeper accumulated sediment than the 15 cm collected in the soil cores, so an irregularity in the ^{210}Pb activity-versus-depth profiles was not anticipated in the natural cores. Because the profile was assumed to represent uninterrupted accumulation, the ^{210}Pb activity-versus-depth profile can itself be used to estimate the rate of sediment accumulation by linear regression on the graph of the natural log of the ^{210}Pb activity over depth (as described in Smoak and Patchineelam 1999). The sediment accumulation rate was calculated using the following equation (simplified from Smoak and Patchineelam 1999):

Equation 4: $$S = \lambda * m$$

where S is the rate of sediment accumulation in millimeters per year (mm/yr), λ is the decay constant of ^{210}Pb (the natural log of 2 divided by the half-life; ln(2)/22.3 in units of /yr), and m is the slope of the linear regression of the graph of the natural log of the ^{210}Pb activity over depth. The rate of mass accumulation in grams per centimeter squared per year ($g/cm^2/yr$) was calculated using the same equation, replacing the depth factor with mass depth (the sum of the dry bulk density in grams per centimeter cubed at a given depth times the 1 cm subsection thickness and every subsection above it in the core, units of grams per square centimeter). The rate of OC accumulation was calculated using the density of OC in grams per centimeter cubed in place of the dry bulk density to calculate OC mass depth for use in Equation 4.

G. Statistical Analyses

All statistical analyses were conducted in IBM SPSS Statistics 26 and graphed in Microsoft Excel for Office 365 (Version 16.0.12527.21296). To evaluate whether the restored forests are approaching equivalence with the natural forests, the mean values of the restored plots for each measurement were plotted against the time since the site's restoration was completed. Values for all the natural sites were averaged to create a single mean reference value. Finally, a time to equivalence (t_{eq}) was calculated for each measurement by setting the regression equation for the restored forest equal to the mean reference value (Osland et al. 2012):

$$t_{eq} = \text{mean reference value / slope of the restored forest regression}$$

Two-way ANOVA was used to evaluate all the environmental variables (hydroperiod and TN) across site and forest management type. To test the assumption that natural sites were sufficiently equivalent to one another to be averaged for comparison to the restored sites, I used a single factor ANOVA to evaluate the mean difference in the values of all response variables. Linear regression was also used to evaluate the relationship between the C pools of natural sites and the environmental variables, soil TN, and hydrology, to determine if these environmental variables explained the variation among natural sites.

Because the sites were cleared of all vegetation prior to planting, any measurement representing the physical biomass (aboveground or belowground) at the time of planting was inferred to be zero ($t = 0$; as measured in terms of trees with DBH $\geq$ 2.5) with regression model fit through the origin. Soil OC did not use this assumption, as the restoration sites varied in soil OC content at planting according to the qualities of the planting soil. Baseline soil OC must therefore be assumed to be an unknown non-zero value.

3. Results

A. Hydrology

Water levels recorded by the gauges over the course of the study ranged from 0.36 m below to 0.50 m above the soil surface (Figure 3). After applying the offsets to the manual wells, water levels at all wells ranged from 0.41 m below to 0.69 m above the soil surface. The maximum water level of HVKB unexpectedly flattened at approximately 0.6 m.

Hydroperiod for each forest management type ("type," natural and restored) was characterized in terms of frequency and duration of flooding at each plot (Figure 4). Flood frequency ranged from 5.8 to 627.1 floods per year in the restored sites (mean ± SE: 231.2 ± 55.6), and from 0 to 611.9 floods per year in the natural sites (158.1 ± 62.8). Flood duration ranged from 4,631 hours to 8,672 hours per year in the restored sites (7,044 ± 390) and from 0 to 8,746 hours per year in the natural sites (5071 ± 1063). Two plots were not submerged at any point over the course of the study (HVKB_NAT_1 and HVKB_NAT 2), which was interpreted to indicate a hydrological disturbance (perhaps historical fill that disrupted the hydrology but did not kill off the existing mangroves).

Flood frequency and flood duration varied by both site and forest management type. The interaction between site and type was significant for flood frequency [2-way ANOVA; $F(3,16) = 9.426$, $p = 0.001$] and flood duration [$F(3,16) = 13.969$, $p < 0.001$]. Significant differences were found among sites in mean flood frequency [1-way ANOVA; $F(3,16) = 4.739$, $p = 0.015$] and flood duration [$F(3,16) = 13.496$, $p < 0.001$]. Tukey's post hoc test showed BBCF differed significantly from NPVK in flood frequency ($p < 0.05$), but neither site was significantly different from the other two sites. Tukey's post hoc test showed the sites divided into two distinct groups in flood duration, with BBCF and HVKB significantly greater ($p < 0.05$) than NPVK and ORSP. The effect of forest management type was significant for flood duration [$F(3,16) = 13.557$, $p = 0.002$] but not flood frequency [$F(3,16) = 2.02$, $p = 0.174$].

One-way ANOVA showed natural sites differed significantly in flood frequency [$F(3,8) = 14.061$, $p = 0.001$] and flood duration [$F(3,8) = 25.919$, $p < 0.001$]. For flood frequency, Tukey's post hoc test showed BBCF differed from the other natural sites ($p < 0.05$) with significantly greater flood frequency (mean ± SE of 487.6 ± 83.1 floods per year, versus 48.0 ± 24.8 floods per year for the other natural sites). For flood duration, Tukey's post hoc analysis showed the natural site hydrology data could be differentiated into two groups ($p < 0.05$), with HVKB and BBCF submerged for relatively few hours per year (1730 ± 687 hours) and NPVK and ORSP submerged for almost every hour of the year (8412 ± 197 hours, or 96% of the entire year).

The restored sites did not differ significantly in flood frequency [($F(3,8) = 3.692$, $p > 0.05$] or flood duration [$F(3,8) = 1.271$, $p > 0.05$)]. None of the restored-natural pairs differed significantly in flood frequency, and only BBCF differed significantly in flood duration [$t(2) = 5.932$, $p < 0.05$].

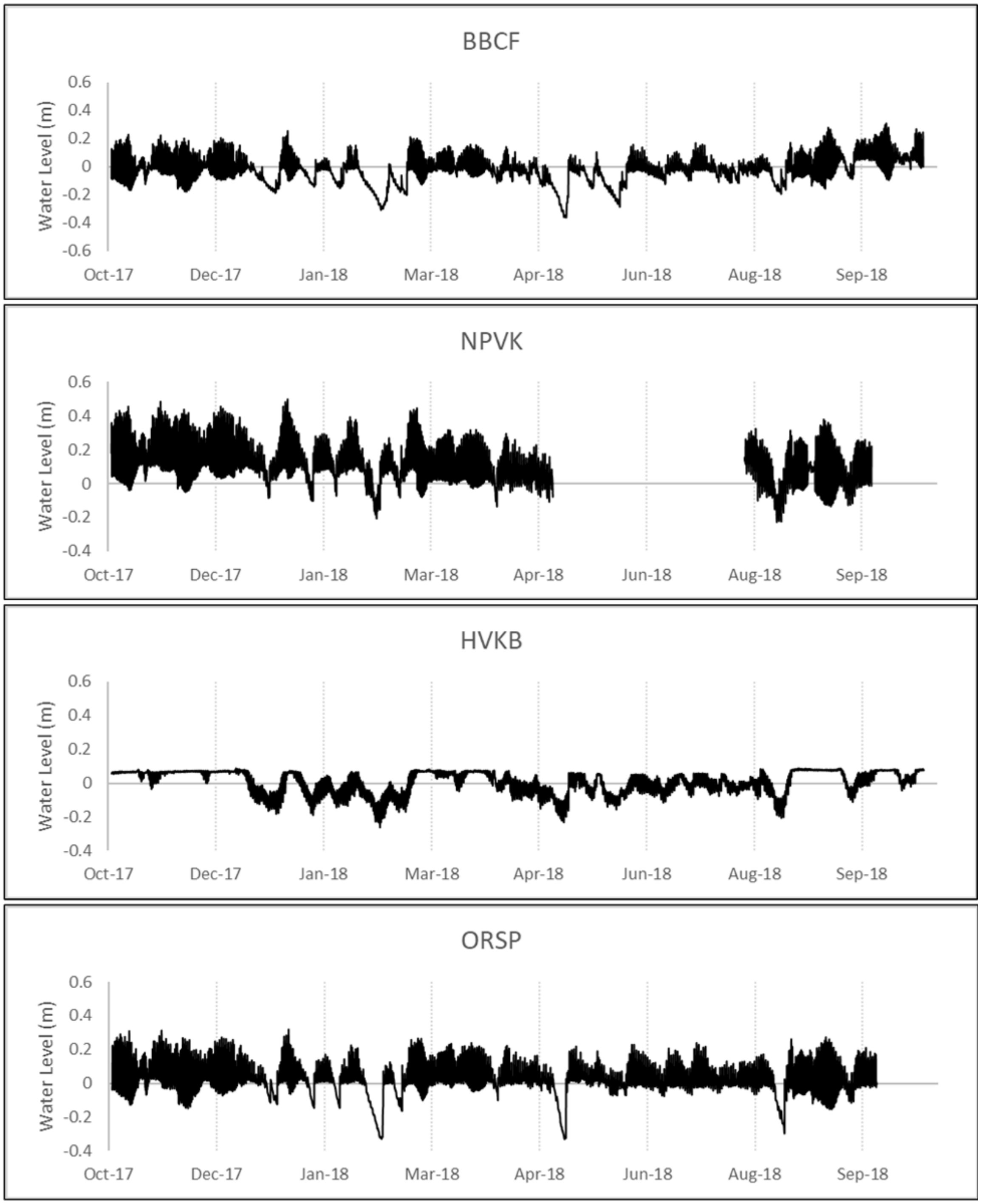

Figure 3: Hydrographs of Restored Sites. Water levels recorded using Onset HOBO pressure gauges. Water level is measured in meters above ground level, where 0 m = soil surface.

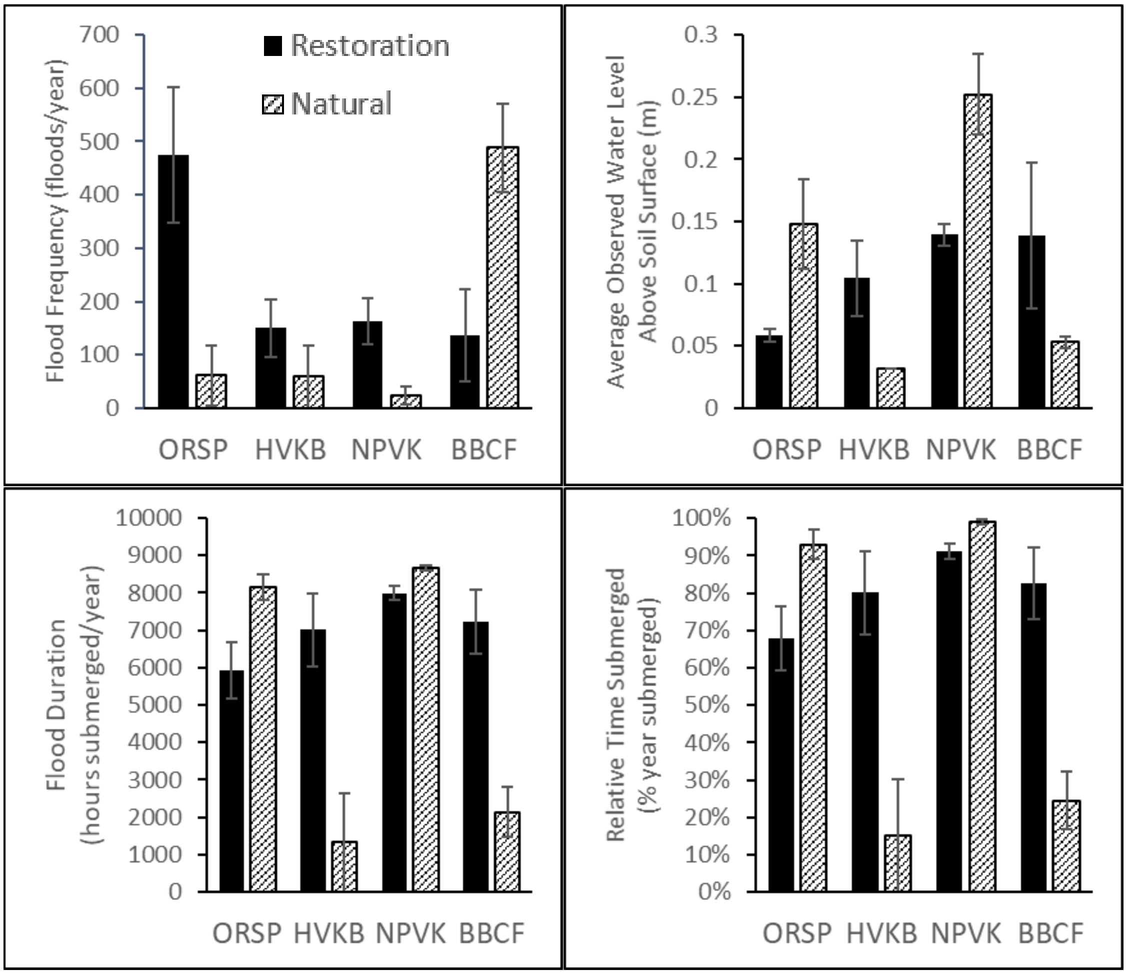

Figure 4: Average Annual Hydroperiod at Each Natural and Restored Site. Data are means with standard error. Sites are Oleta River State Park (ORSP), Historic Virginia Key Beach Park (HVKB), North Point Virginia Key (NPVK), and Bill Baggs Cape Florida State Park (BBCF). Flood frequency recorded as independent occurrences of surface submergence (floods per year), and flood duration recorded as the sum of all time during which the soil surface was submerged over the course of one year (flood duration).

Table 3: Forest Structure Characteristics by Species. Black (B), red (R), and white (W) mangroves were observed. Data are mean ± standard error. Values marked with a single asterisk (*) indicate a species was observed in only one plot from that site and management type. Values marked with a double asterisk (**) indicate a species was not found in any plot for that site and management type.

Site	Species	Density (stems/ha)	Basal Area (m2/ha)	Average DBH (cm)	Max DBH (cm)	Average Height (m)	Max Height (m)
BBCF_REST	B	400 ± 351	0.82 ± 0.78	4.1 ± 1	4.8 ± 1.7	4.2 ± 0.8	4.8 ± 1.5
	R	7500 ± 3079	8.91 ± 4.21	3.7 ± 0.2	5.9 ± 0.7	5.4 ± 0.7	7 ± 1
	W	567 ± 318	0.47 ± 0.29	3.2 ± 0.2	4.2 ± 0.7	4.3 ± 0.4	5.2 ± 0.7
BBCF_NAT	B	967 ± 570	4.97 ± 0.62	9.5 ± 2.8	16 ± 4.8	6.7 ± 0.6	9.4 ± 0.8
	R	3067 ± 333	13.5 ± 2.13	6.6 ± 0.2	15.1 ± 1.1	7 ± 0.1	10.6 ± 0.6
	W	333 ± 120	3.64 ± 2.2	11.5 ± 3.5	15 ± 4.1	9.3 ± 1.9	11.2 ± 1.6
HVKB_REST	B	67 ± 67	0.05 ± 0.05	3*	3.5*	4.6*	5.3*
	R	3433 ± 1431	2.5 ± 1.12	3 ± 0.1	3.8 ± 0.1	4.5 ± 0.3	5.6 ± 0.5
	W	133 ± 133	0.08 ± 0.08	2.8*	3*	4.5*	4.8*
HVKB_NAT	B	600 ± 600	0.56 ± 0.56	3.4*	4.6*	5.6*	7.2*
	R	2133 ± 984	20.69 ± 9.02	12.7 ± 4.8	18.7 ± 6.8	10.2 ± 2.1	12.3 ± 2.2
	W	1433 ± 1335	1.29 ± 0.92	5.1 ± 2	6.2 ± 2.2	7.3 ± 2.3	9 ± 2.8
NPVK_REST	B	400 ± 100	0.39 ± 0.12	3.4 ± 0.3	4.6 ± 0.7	3.8 ± 0.2	4.4 ± 0.1
	R	2700 ± 608	2.75 ± 0.85	3.4 ± 0.1	5.9 ± 0.7	4.8 ± 0.1	7.2 ± 0.7
	W	3100 ± 608	3.18 ± 0.83	3.5 ± 0.1	6 ± 0.8	4.7 ± 0.2	6.6 ± 0.4
NPVK_NAT	B	33 ± 33	0.39 ± 0.39	12.3*	12.3*	9.5*	9.5*
	R	2800 ± 252	19.58 ± 2.25	8.8 ± 0.7	17.4 ± 1.3	9.1 ± 0.2	12 ± 0.2
	W	33 ± 33	0.24 ± 0.24	9.5*	9.5*	11.3*	11.3*
ORSP_REST	B	1233 ± 536	1.07 ± 0.51	3.1 ± 0.2	4.3 ± 0.8	4.3 ± 0.2	5.2 ± 0.3
	R	2267 ± 780	1.37 ± 0.51	2.7 ± 0.1	3.2 ± 0.2	4.4 ± 0.2	4.9 ± 0.2
	W	3167 ± 924	2.37 ± 0.76	3 ± 0.1	4.2 ± 0.3	4.3 ± 0.3	5.2 ± 0.4
ORSP_NAT	B	0 ± 0	0 ± 0	NA**	NA**	NA**	NA**
	R	1767 ± 371	17.86 ± 5.73	10.9 ± 2.2	19.3 ± 2.6	9.7 ± 1.1	13.1 ± 1.2
	W	67 ± 67	0.44 ± 0.44	8.2*	12.3*	5.6*	9.5*

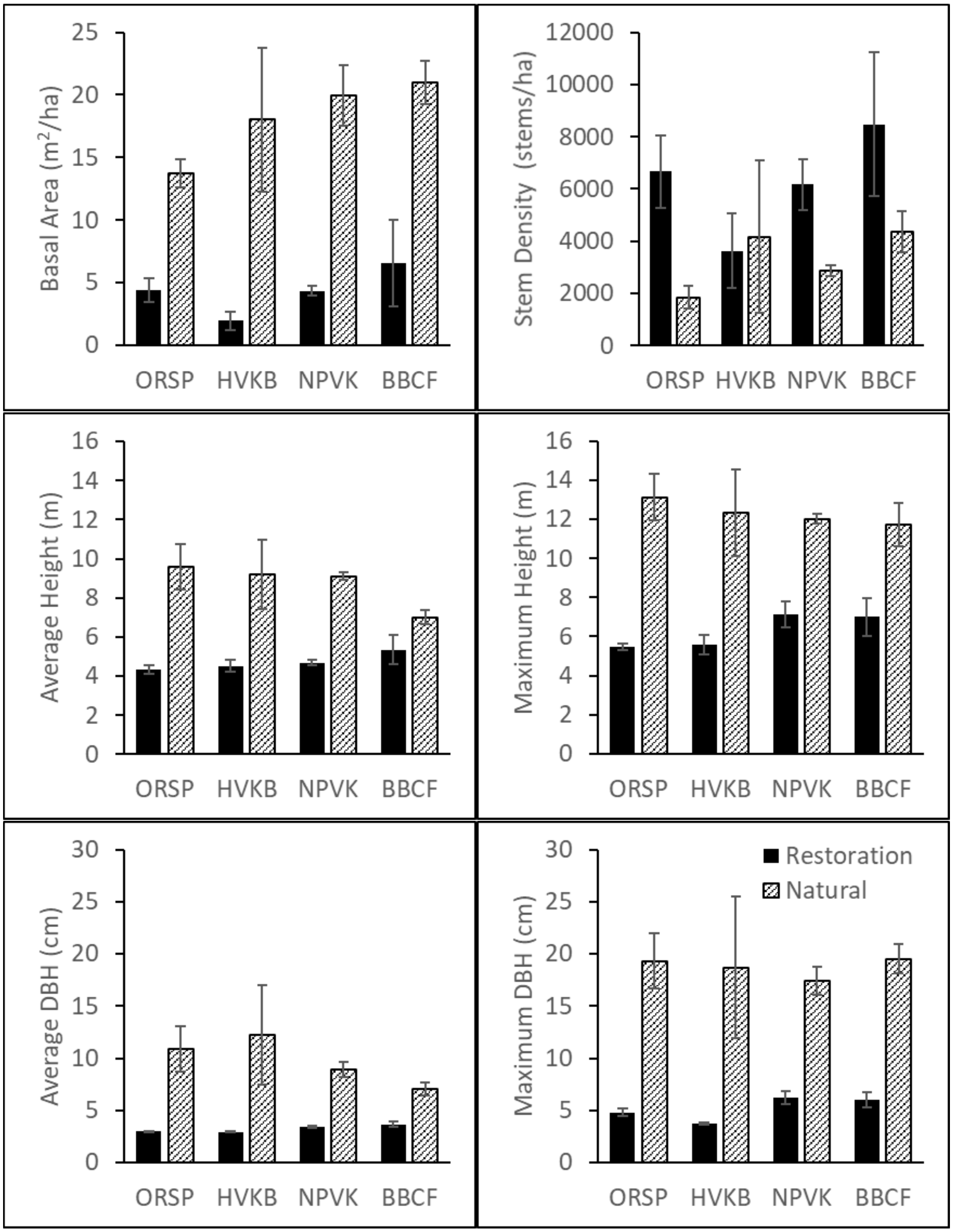

Figure 5: Forest Structure Measurements at Each Natural and Restored Site. Forest structure measurements, from top: basal area in meters squared per hectare; stem density in tagged stems (stems with DBH ≥ 2.5 cm) per hectare; average height in meters; maximum height in meters; average DBH in cm; and maximum DBH in centimeters. All measurements mean ± standard error.

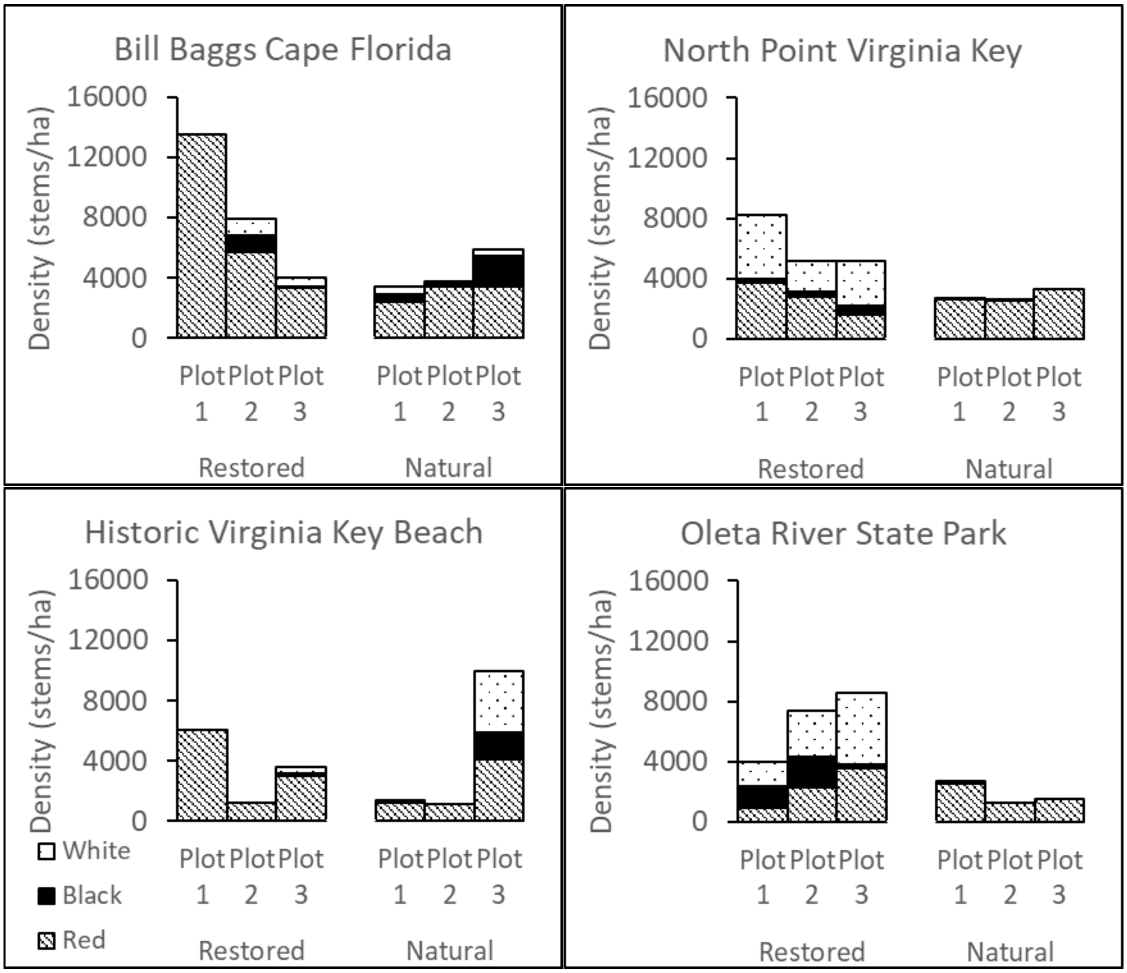

Figure 6: Species Composition at Each Natural and Restored Site. Number of black, red, and white mangroves with DBH ≥ 2.5 cm at each study plot, converted to stems per hectare. Red mangroves are the only species present at every site and are the most numerous species in 18 of the 24 sites.

B. Forest Structure

The average value for basal area, average height, maximum height, average DBH, and maximum DBH was greater in the natural sites as compared to the restored sites (Table 3; Figure 5). Stem density in restored sites, in contrast, was greater than or equal to stem density in natural sites (Table 3, Figure 5).

Red mangroves were the only species present in every study plot, with white mangroves present in 66% of the plots and black mangroves present in 58% of the plots (Figure 6). Red mangroves were the most abundant species in 18 of the 24 plots; white mangroves were the most abundant in five of the remaining plots (ORSP_REST_1-3, NPVK_REST_1, NPVK_REST_3), and in one plot red and white mangroves were equally abundant (HVKB_NAT_3). Natural plots ranged from 1,100 to 4,100 red mangroves per hectare, with up to 2,100 black mangroves and up to 4,100 white mangroves per hectare. Restored plots ranged from 900 to 13,500 red mangroves per hectare, with up to 2,000 black mangroves and up to 4,800 white mangroves per hectare.

Basal area in restoration plots ranged from 0.63 to 13.32 m^2/ha (4.31 ± 0.96), while natural plots ranged from 6.61 to 24.99 m^2/ha (18.18 ± 1.63). I did not find a significant interaction between site and type [$F(3,16) = 0.663$, $p = 0.587$] nor due to site [$F(3,16) = 1.270$, $p = 0.318$]. Mean basal area was significantly higher in the natural sites than the restoration sites [$F(3,16) = 54.346$, $p < 0.001$]. One-way ANOVA did not show a significant difference among the natural sites [$F(3,8) = 0.939$, $p = 0.466$] or the restored sites [$F(3,8) = 1.054$, $p > 0.05$)]. Three of the four restored-natural pairs differed significantly in basal area: BBCF [$t(2) = 4.918$, $p < 0.05$], NPVK [$t(2) = 5.645$, $p < 0.05$], and ORSP [$t(2) = 14.920$, $p < 0.05$].

Stem density ranged from 1,200 stems/ha to 13,500 stems/ha in restored plots (6233 ± 915) and from 1,100 stems/ha to 10,000 stems/ha in natural plots (3308 ± 722). I did not find a significant interaction between site and type [$F(3,16) = 1.048$, $p > 0.05$] nor a significant difference due to site [$F(3,16) = 0.931$, $p > 0.05$]. Mean stem density was significantly greater in the restoration types than the natural types [$F(3,16) = 6.283$, $p < 0.05$]. One-way ANOVA did not show a significant difference among the natural sites [$F(3,8) = 0.603$, $p = 0.631$] or the restored sites [$F(3,8) = 1.280$, $p > 0.05$)]. None of the restored-natural pairs showed a significant difference in stem density.

The average height of all mangroves in the restoration plots ranged from 3.89 m to 6.65 m (6.30 ± 0.36), while the average height in natural mangroves ranged from 5.63 m to 11.27 m (12.30 ± 0.61). I did not find a significant difference among the means in the interaction between site and type [$F(3,16) = 1.899$, $p > 0.05$] nor due to site [$F(3,16) = 0.393$, $p > 0.05$]. The average height of all mangroves was found to be significantly greater in the natural types than the restoration types [$F(3,16) = 47.419$, $p < 0.001$]. One-way ANOVA did not show a significant difference among the natural sites [$F(3,8) = 1.151$, $p > 0.05$] or the restored sites [$F(3,8) = 1.113$, $p > 0.05$)]. Only two of the four restored-natural pairs were significantly different in average height: NPVK [$t(2) = 22.460$, $p < 0.05$] and ORSP [$t(2) = 5.727$, $p < 0.05$].

The maximum height for restored mangroves ranged from 4.55 m to 8.44 m (4.73 ± 0.21), and the maximum height in the natural mangroves ranged from 7.9 m to 15.1 m (8.73 ± 0.55). I did not find a significant difference among the means from the interaction between site and type [$F(3,16) = 0.894$, $p > 0.05$], nor due to site [$F(3,16) = 0.116$, $p > 0.05$]. The maximum mangrove height in the natural types was found to be significantly greater than in the restoration types [$F(3,16) = 61.640$, $p < 0.001$]. One-way ANOVA did not show a significant difference among the natural sites [$F(3,8) = 0.191$, p > 0.05] or the restored sites [$F(3,8) = 1.942$, $p > 0.05$)]. Three of the restored-natural pairs were significantly different: BBCF [$t(2) = 15.560$, $p < 0.05$], NPVK [$t(2) = 10.799$, $p < 0.05$], and ORSP [$t(2) = 7.004$, $p < 0.05$]

Average DBH in restored mangroves ranged from 2.8 to 3.9 cm (3.3 ± 0.1), while the average DBH in natural forests ranged from 3.3 to 19.5 cm (9.8 ± 1.3). I did not find a significant interaction between site and type [$F(3,16) = 0.966$, $p > 0.05$], nor did I find a significant difference among the means due to site [$F(3,16) = 0.517$, $p > 0.05$]. Average DBH was significantly greater in the natural types than in the restoration types [$F(3,16) = 23.765$, $p < 0.001$]. One-way ANOVA did not show a significant difference among the natural sites [$F(3,8) = 0.725$, $p > 0.05$], but did show a significant difference among the restoration sites [$F(3,8) = 6.360$, $p < 0.05$)]. Tukey's post-hoc analysis identified two subgroups, with HVKB_REST and ORSP_REST in one subgroup, BBCF_REST in the other subgroup, and NPVK_REST in both subgroups. Two of the four restored-natural pairs were significantly different: BBCF [$t(2) = 9.572$, $p < 0.05$] and NPVK [$t(2) = 6.561$, $p < 0.05$].

Maximum DBH in restored forests ranged from 3.5 to 7.4 cm (5.185 ± 0.374), and maximum DBH in natural forests ranged from 5.4 to 27.9 cm (18.746 ± 1.626). I did not find a significant interaction between site and type [$F(3,16) = 0.190$, $p > 0.05$], nor due to site [$F(3,16) = 0.112$, $p > 0.05$]. Maximum DBH was significantly higher in the natural types than in the restoration types [$F(3,16) = 50.755$, $p < 0.001$]. One-way ANOVA did not show a significant difference among the natural sites [$F(3,8) = 0.063$, $p > 0.05$], but did show a significant difference among the restoration sites [$F(3,8) = 4.670$, $p < 0.05$]. Tukey's post-hoc analysis identified two subgroups, with HVKB_REST in one subgroup, NPVK_REST in another, and ORSP_REST and BBCF_REST in both subgroups. Three of the restored-natural pairs differed significantly: BBCF [$t(2) = 19.377$, $p < 0.05$], NPVK [$t(2) = 5.667$, $p < 0.05$], and ORSP [$t(2) = 5.308$, $p < 0.05$].

Linear regression analyses were used to estimate the time for each forest structure measurement to reach equivalence to the mean reference values derived from the natural sites (Figure 7, Table 4). All six forest structure measurements demonstrated a strong, significant relationship ($r^2 > 0.90$, $p < 0.05$). The t_{eq} values varied widely, from 7.8 years for stem density to 59.7 years for basal area. Besides stem density, none of the forest structure values had reached equivalence after 20 years (Table 4).

Table 4: Forest Structure Regression Values. Key measurements from the regression for each measurement of forest structure over time since restoration. Mean reference value, time to equivalence (t_{eq}*),* r^2*, and* p*-value are provided.*

Measure	Mean Reference Value	Mean Restoration Value	t_{eq} (years)	r^2	*p*-value
Basal Area (m^2/ha)	18.20 ± 5.60	4.31 ± 0.93	62.7	0.916	0.007
Stem Density (mangroves/ha)	3308 ± 722	6233 ± 915	8.13	0.914	0.007
Average DBH (cm)	9.8 ± 1.3 cm	3.3 ± 0.1 cm	47	0.932	0.005
Max DBH (cm)	18.7 ± 1.6 cm	5.2 ± 0.4 cm	55.3	0.954	0.003
Average Tree Height (m)	8.7 ± 0.6 m	4.7 ± 0.2 m	29.2	0.916	0.007
Max Tree Height (m)	12.3 ± 0.6 m	6.3 ± 0.4 m	30.3	0.945	0.004

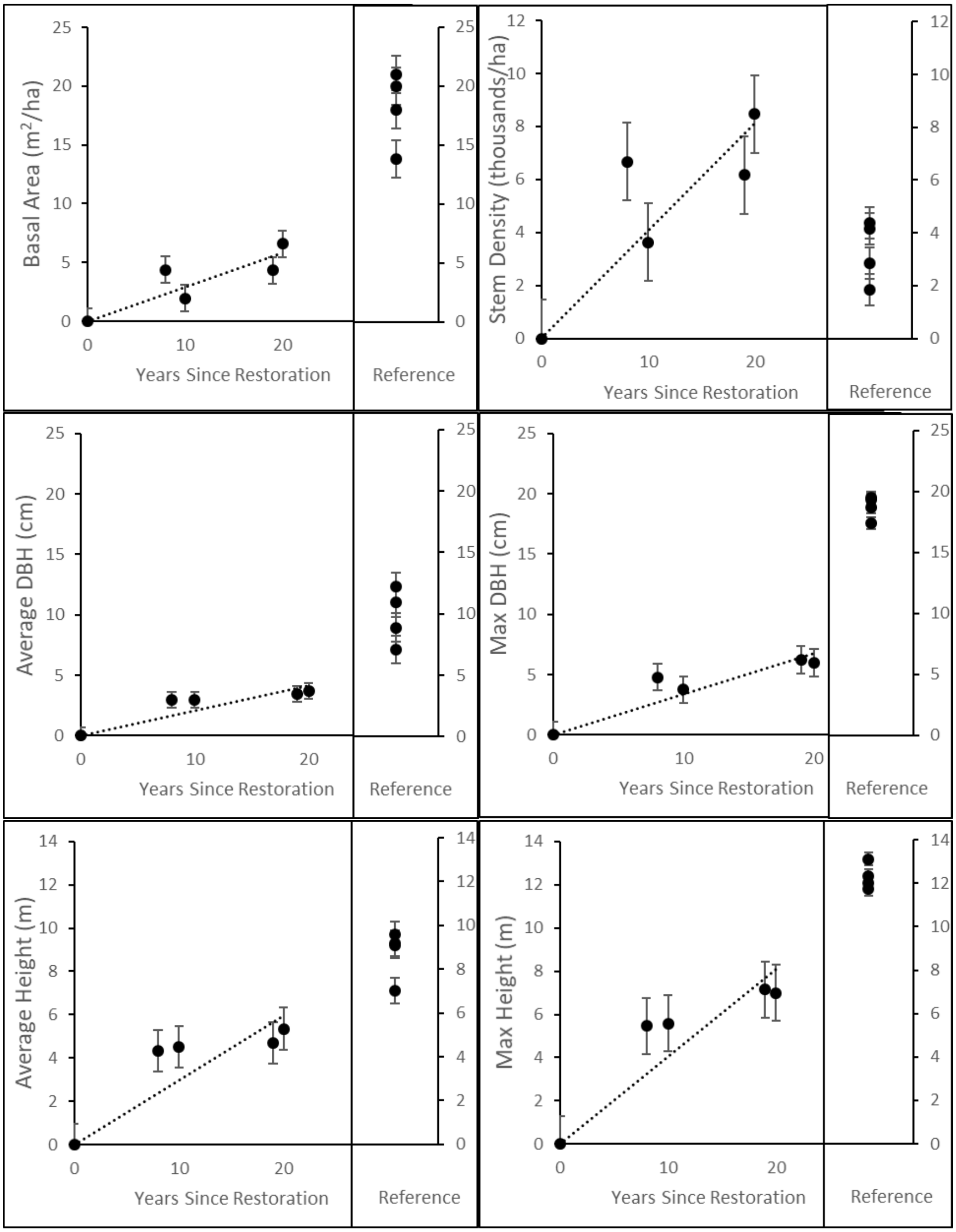

Figure 7: Regression of Forest Structure Measurements over Time. Restoration values are graphed on the x axis at the time since restoration was completed (in years), while the natural sites are all graphed to the right of the regression over time. Forest structure measurements, from top: basal area in meters squared per hectare; stem density in tagged stems (stems with DBH ≥ 2.5 cm) per hectare; average height in meters; maximum height in meters; average DBH in cm; and maximum DBH in centimeters.

C. Carbon Storage

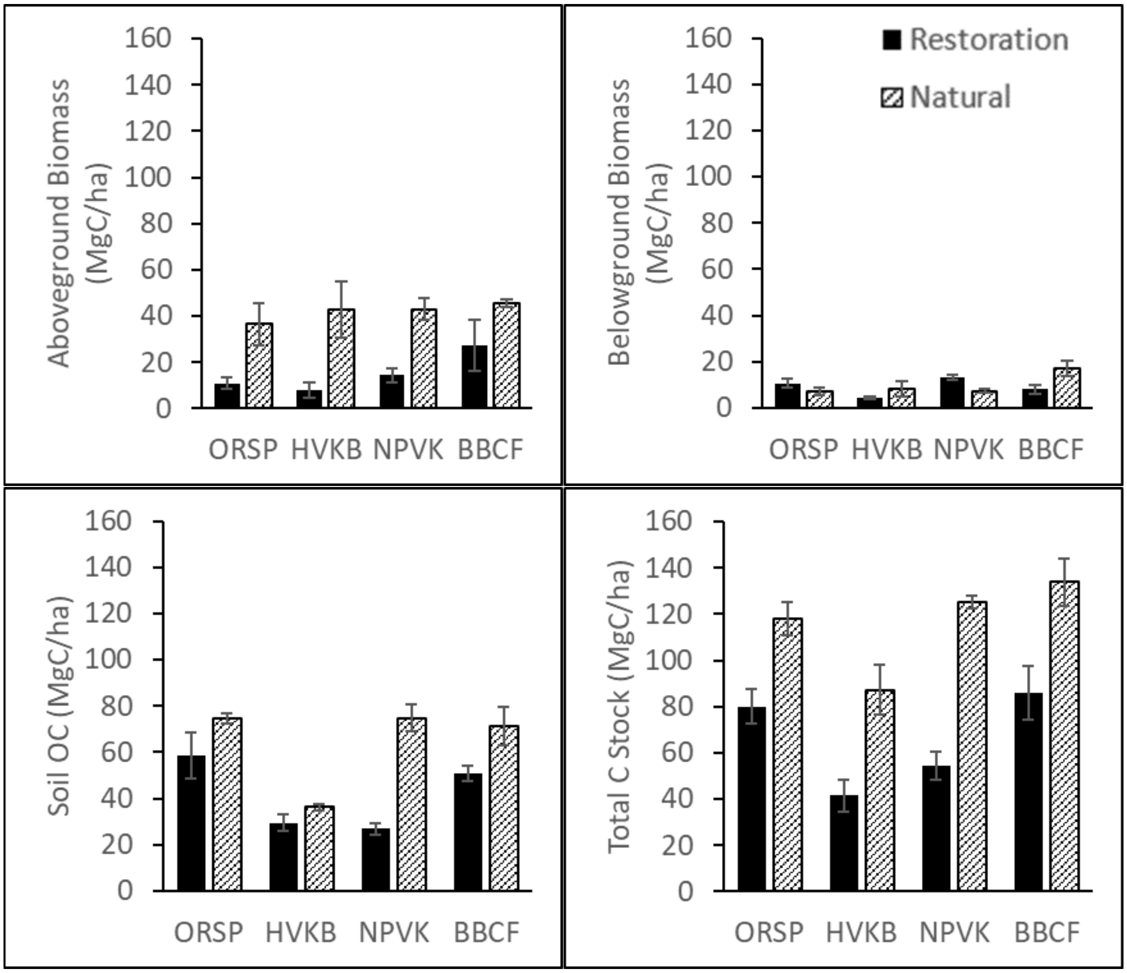

Figure 8: Carbon Storage at Each Natural and Restoration Site. Data are means with standard error. From top: aboveground biomass; belowground biomass; soil OC; and C stock (sum of the three pools), all in megagrams C per hectare.

Table 5: Carbon Storage Regression Values. Key measurements from the regression for each C pool. Mean reference value, mean restoration value, time to equivalence in years (t_{eq}), r^2, *and* p-*value are provided.*

C Pool	Mean Reference Value (MgC/ha)	Mean Restoration Value (MgC/ha)	t_{eq} (years)	r^2	*p*-value
Aboveground Biomass	41.99 ± 3.53	15.05 ± 3.41	50.4	0.948	0.018
Belowground Biomass	9.89 ± 1.63	9.09 ± 1.16	13.6	0.895	0.036
Soil OC	64.17 ± 5.39	41.36 ± 4.74	NA	0.059	0.757
Total C Stock	116.05 ± 6.41	65.50 ± 6.55	NA	0.041	0.799

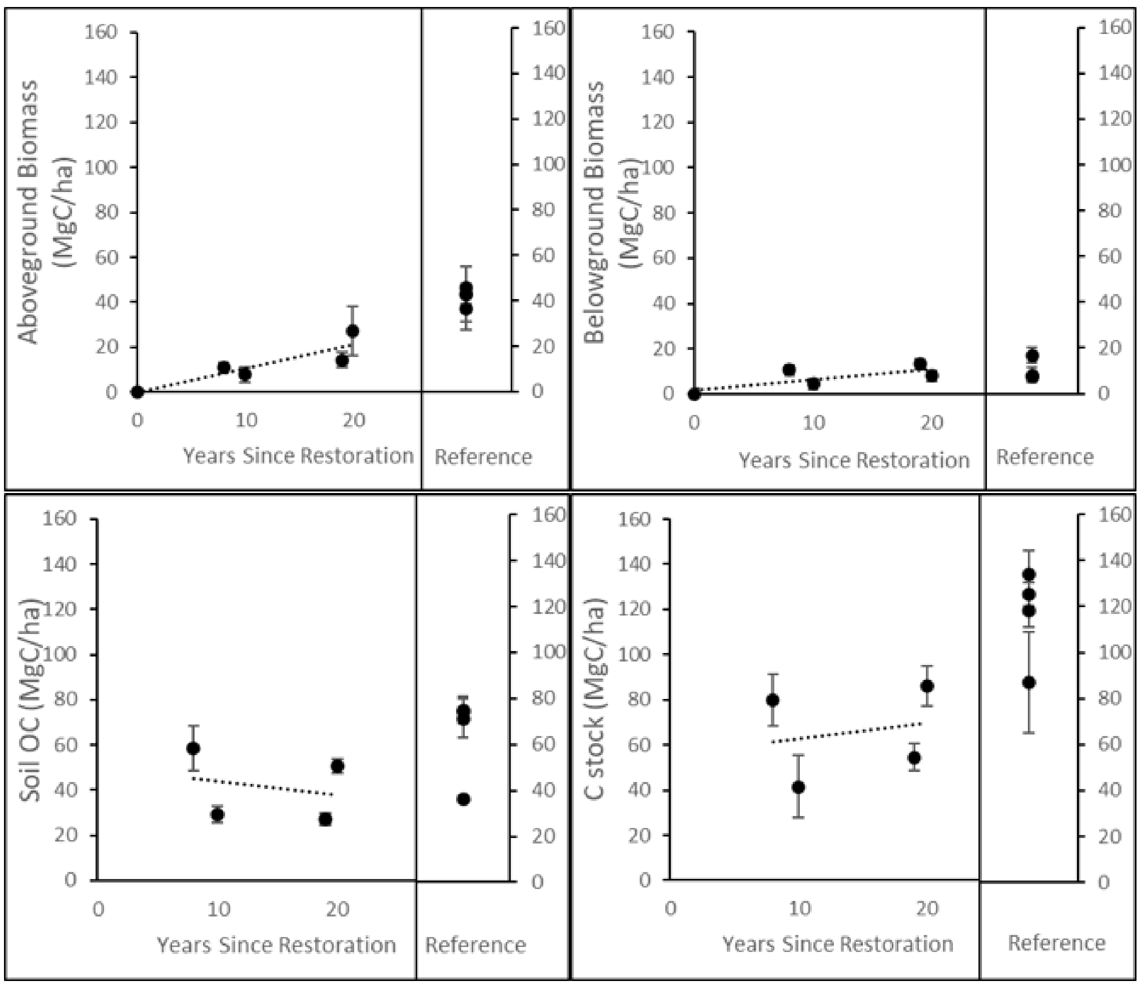

Figure 9: Regression of Carbon Storage over Time. Restoration values graphed on the x axis at the time since restoration was completed (in years), while the natural sites are all graphed to the right of the regression over time. From top: aboveground biomass; belowground biomass; soil OC; and C stock (sum of the three pools), all in megagrams C per hectare (MgC/ha). All values with standard error.

D. Carbon Storage in Aboveground Biomass

The C stored in aboveground biomass (AGB) at the restoration sites ranged from 2.26 to 46.77 MgC/ha (15.06 ± 3.41) and at natural sites ranged from 20.58 to 62.16 MgC/ha (41.99 ± 3.54) (Figure 8). I applied two-way ANOVA to test whether C differed by site or type and did not find a significant interaction of site and type [$F(3,16) = 0.472$, $p > 0.05$] nor from the effects of site [$F(3,16) = 1.303$, $p > 0.05$]. The C stored in AGB was found to be significantly greater in the natural sites than the restoration sites [$F(3,16) = 29.109$, $p < 0.001$]. One-way ANOVA did not indicate a significant difference in mean aboveground biomass among natural reference sites [$F(3,8) = 0.239$, $p > 0.05$] or restored sites [$F(3,8) = 2.001$, $p > 0.05$]. A significant difference was not found between any of the restored-natural site pairs.

The mean reference value was 41.99 MgC/ha. Under the inference conditions ($t = 0$, AGB = 0, with regression forced through the origin), linear regression analysis showed a strong positive relationship over time ($r^2 = 0.946$ and $p < 0.05$). The $t_{eq} = 50.4$ years (Table 5, Figure 9).

E. Carbon Storage in Belowground Biomass

Belowground biomass (BGB) ranged from 3.57 to 14.96 MgC/ha (9.09 ± 1.16) at the restoration sites and from 2.79 to 23.53 MgC/ha (9.89 ± 1.63) at the natural sites. There was a significant interaction between site and type [$F(3,16) = 5.384$, $p < 0.05$]. No significant difference was found due to the effects of site alone [$F(3,16) = 3.150$, $p > 0.05$] or type alone [$F(3,16) = 0.303$, $p > 0.05$]. One-way ANOVA did not indicate a significant difference in belowground biomass among natural sites [$F(3,8) = 3.364$, $p >$

0.05], but a significant difference was found among restoration sites [$F(3,8) = 7.186$, $p <$ 0.05]. Tukey's post-hoc analysis identified two subgroups within the data, one containing HVKB_REST, another containing NPVK_REST, with BBCF_REST and ORSP_REST in both subgroups. Of the restored-natural site pairs, only two were significantly different: BBCF [$t(2) = 5.731$, $p < 0.05$] and NPVK [$t(2) = 28.993$, $p < 0.05$].

The mean reference value for C in belowground biomass was 9.89 MgC/ha. Under the inference conditions, there was a strong, positive relationship for belowground biomass in the restored sites as belowground biomass increased over time ($r^2 = 0.895$ and $p < 0.05$) (Table 5; Figure 9). The $t_{eq} = 13.6$ years.

F. Soil Carbon Storage

Soil organic C (OC) ranged from 21.75 to 78.01 MgC/ha (41.36 ± 4.74) in restoration sites and from 33.41 to 86.68 MgC/ha (64.17 ± 5.40) in the natural sites. There was not a significant interaction between site and type; however, a significant difference was found due to the effects of site alone [$F(3,16) = 14.469$, $p < 0.001$] and type alone [$F(3,16) = 34.347$, $p < 0.001$]. One-way ANOVA of the soil OC of the natural sites indicated one of the natural sites differed significantly from the other natural sites [$F(3,8) = 12.233$, $p < 0.05$]; Tukey's post hoc test confirmed the soil OC at HVKB_NAT to be significantly lower than at the other three natural sites with a mean soil OC of 36.18 ± 1.43 MgC/ha versus 73.50 ± 3.11. A significant difference was also found among the restored sites [$F(3,8) = 7.643$, $p < 0.05$]. Tukey's post hoc test identified two subgroups, with NPVK_REST in one subgroup and ORSP_REST in the other, with BBCF_REST and HVKB_REST in both subgroups. Only NPVK differed significantly between the restoration and natural sites [$t(2) = 9.533$, $p < 0.05$]. Dry bulk density, soil OC, and soil IC were also graphed over depth (Figure 10, Figure 11, Figure 12, respectively); no consistent trend over depth was observed among sites, forest management types, or restored-natural pairs.

The mean reference value derived from the natural sites was 64.166 MgC/ha. Soil OC cannot be assumed to have a value of 0 at time $t = 0$, because the OC of the initial planting soil is not known, so inference conditions could not be used for soil OC; accordingly, the regression was not forced to pass through the origin. No relationship was found between mean soil OC and time ($r^2 = 0.059$, $p > 0.05$) (Table 5; Figure 9); therefore, t_{eq} could not be calculated.

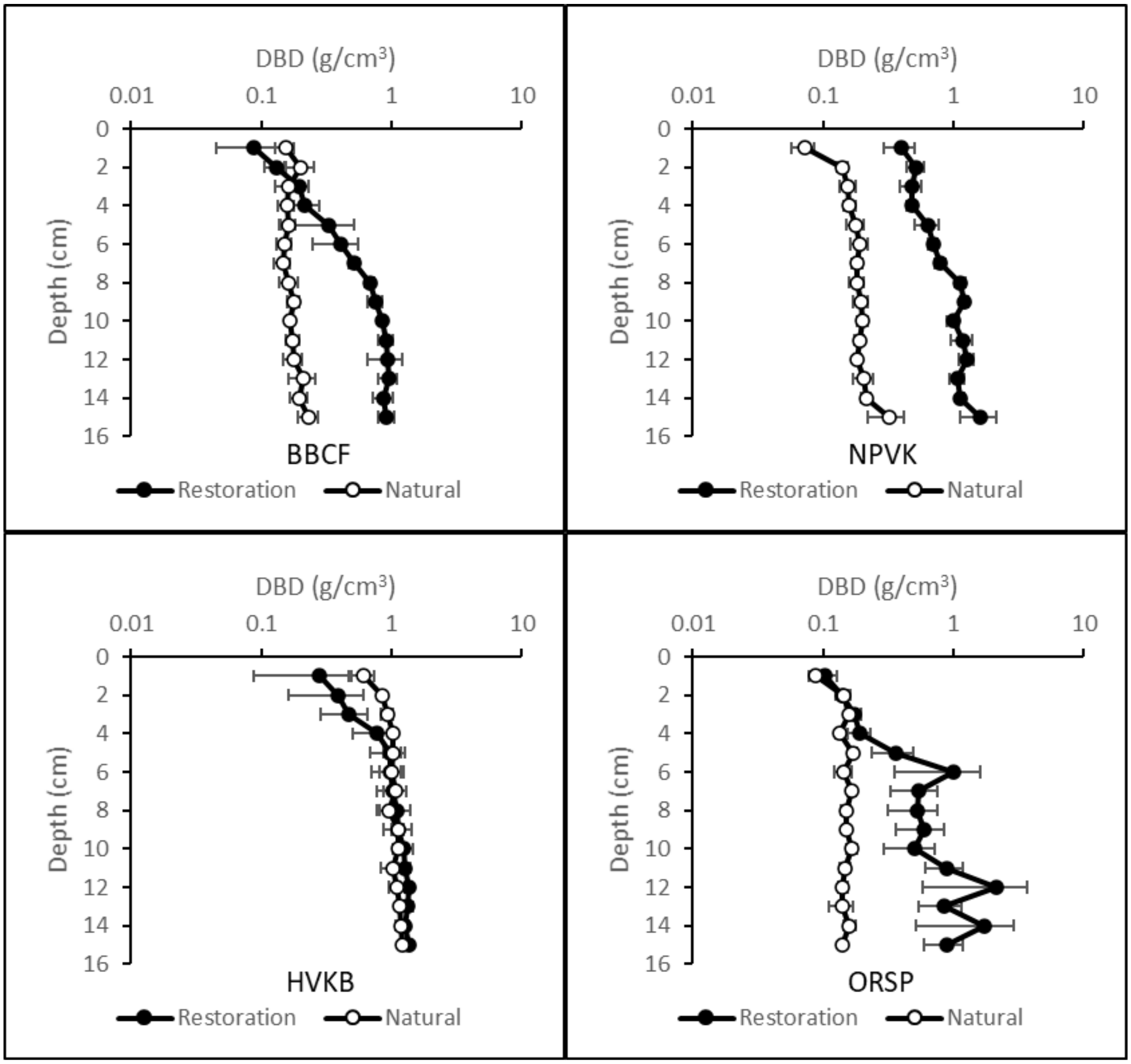

Figure 10: Dry Bulk Density over Depth. Dry bulk density (g/cm^3) over depth (cm) for restored and natural soil cores at all four study sites. All values are mean ± SE.

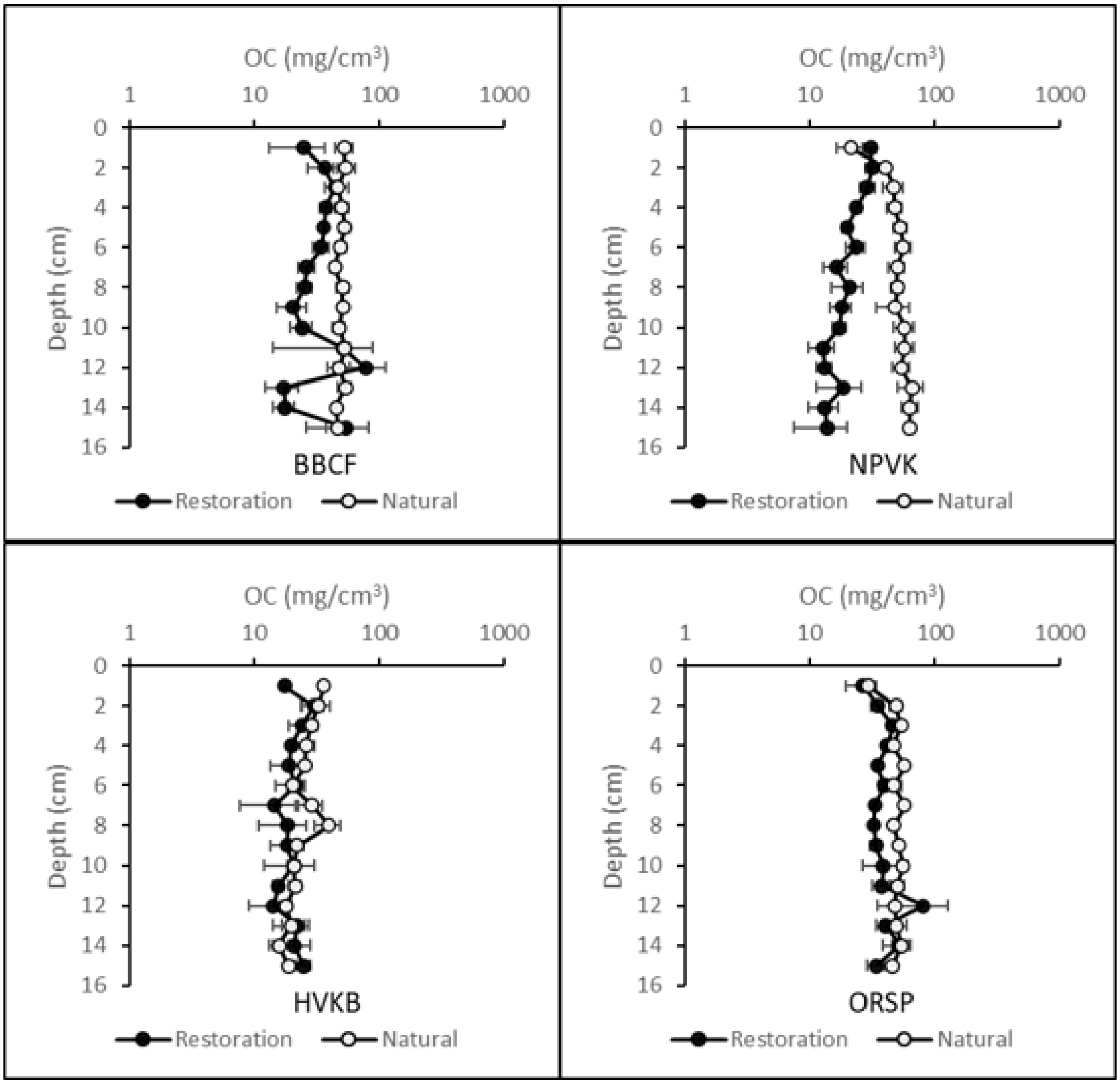

Figure 11: Soil Organic Carbon over Depth. Soil organic carbon (mg/cm^3) over depth (cm) for restored and natural cores at all four study sites. All values are mean ± SE.

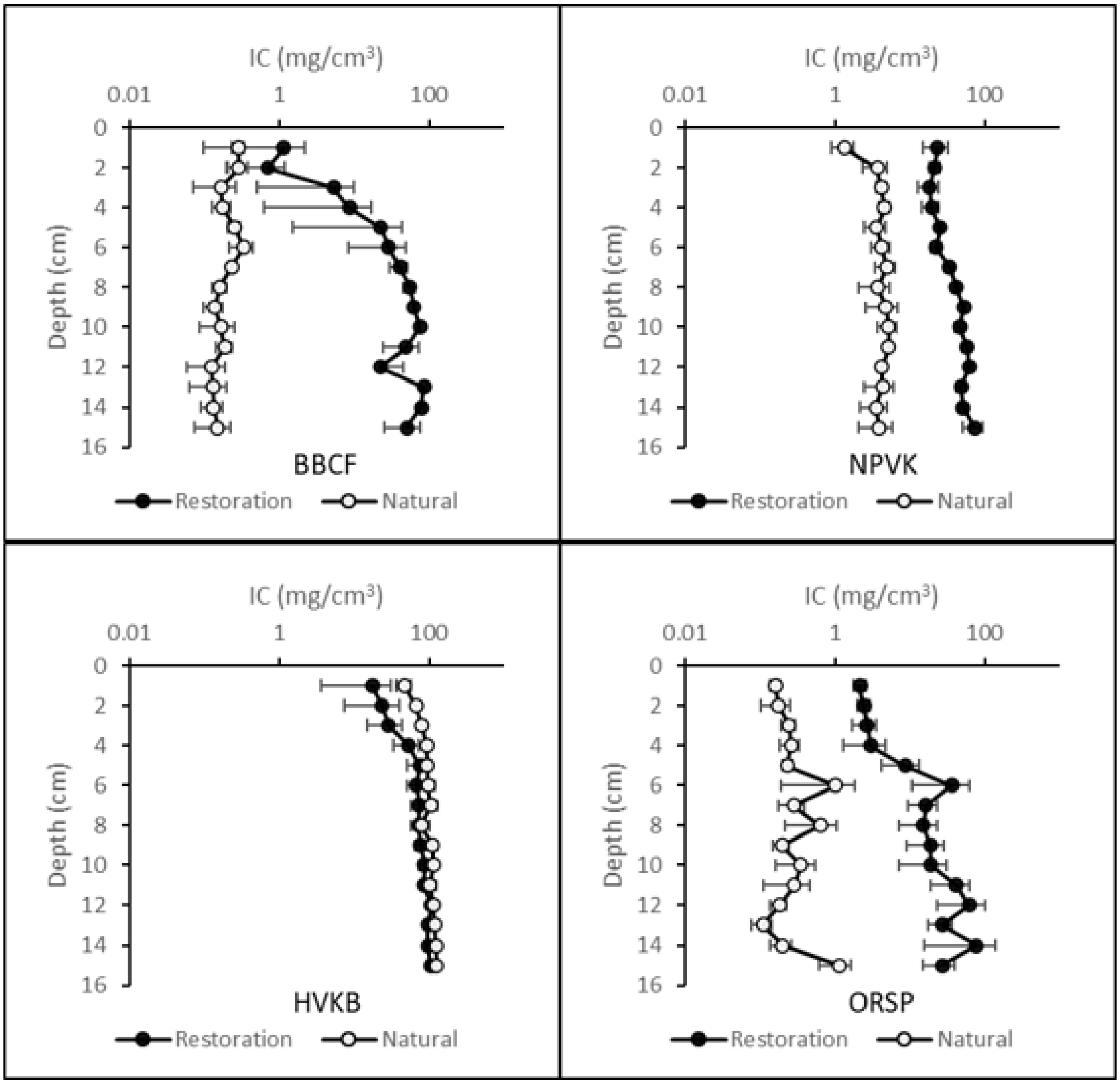

Figure 12: Soil Inorganic Carbon over Depth. Soil inorganic carbon content (mg/cm^3) over depth (cm) for restored and natural cores at all four study sites. All values are mean ± SE.

G. Soil TN

Soil TN was characterized by area in megagrams of TN per hectare (Mg/ha) and by mass in grams TN per kilogram (g/kg) (Figure 13). Soil TN in restoration sites ranged from 1.213 to 3.429 Mg/ha by area (2.092 ± 0.163) and 0.923 to 8.639 g/kg by mass

(2.686 ± 0.619), while soil TN in natural sites ranged from 2.363 to 4.202 Mg/ha by area (3.241 ± 0.172) and 1.393 to 15.924 g/kg by mass (11.314 ± 1.695).

Mean soil TN by area among all sites differed by forest management type but not by site. There was a significant interaction between site and type [$F(3,16) = 4.510$, $p = 0.018$]. The effect of type was also significant in soil TN by area [$F(3,16) = 38.812$, $p < 0.001$] but there was not a significant difference by site.

One-way ANOVA was applied in the natural sites to test whether soil TN by area differed among sites, and a significant difference was found [$F(3,8) = 4.206$, $p = 0.046$]. Tukey's post-hoc test showed HVKB_NAT was distinct from NPVK_NAT, with a mean soil TN by area of 2.490 ± 0.089 Mg/ha, versus a soil TN for NPVK_NAT of 3.661 ± 0.285 Mg/ha. Neither HVKB_NAT nor NPVK_NAT differed significantly from the other two natural sites. One-way ANOVA did not indicate a significant difference among the restored sites [$F(3,8) = 2.685$, $p > 0.05$)]. Of the natural-restored pairs (Figure 13), only NPVK had a significant difference in soil TN by area [$t(2) = 17.549$, $p < 0.05$]. Soil TN was also graphed over depth (Figure 14).

Sites differed by both site and type in soil TN by mass. There was a significant interaction between site and type indicating differing means for soil TN by area [$F(3,16) = 27.499$, $p < 0.001$]. The effect of site and type individually were also significant in soil TN by mass [$F(3,16) = 44.766$ and 241.846, respectively; for both, $p < 0.001$]. One-way ANOVA was applied in the natural sites to test whether soil TN differed by mass, and a significant difference was found [$F(3,8) = 110.740$, $p < 0.001$]. Tukey's post-hoc test showed the natural sites at HVKB are distinct from all other sites, with a mean soil TN by mass of 1.706 ± 0.219 g/kg versus the mean soil TN of the other natural sites, for which mean soil TN was14.517 ± 0.371 g/kg. One-way ANOVA did not indicate a significant difference among the restored sites [$F(3,8) = 3.870$, $p > 0.05$)]. Three of the natural-restored pairs differed significantly in soil TN by mass: ORSP [$t(2) = 7.599$, $p < 0.05$], NPVK [$t(2) = 60.659$, $p < 0.05$], and BBCF [$t(2) = 4.894$, $p < 0.05$].

To understand why soil OC at HVKB_NAT differed from the other natural sites, the relationship between soil OC and hydrology and soil TN were evaluated by linear regression. For the four natural sites, there was no linear relationship between flood frequency and soil OC ($r^2 = 0.039$, $p > 0.05$) (Figure 15). For flood duration versus soil OC, the four sites together had a significant relationship of moderate magnitude ($r^2 = 0.423$, $p < 0.05$). Soil OC and soil TN had a strong linear relationship across both measurements of soil TN in the natural sites (Figure 16); for soil TN in MgC/ha, $r^2 = 0.879$, $p < 0.05$; for soil TN in g/kg, $r^2 = 0.788$, $p < 0.05$).

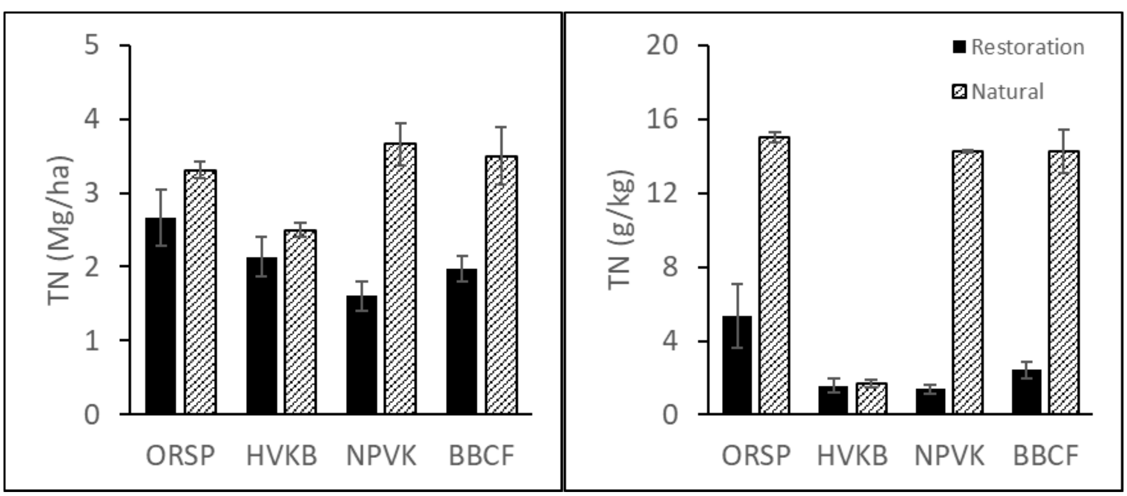

Figure 13: Soil TN at Each Natural and Restored Site. Data are means with standard error, measured in megagrams per hectare (left) and grams per kilogram (right).

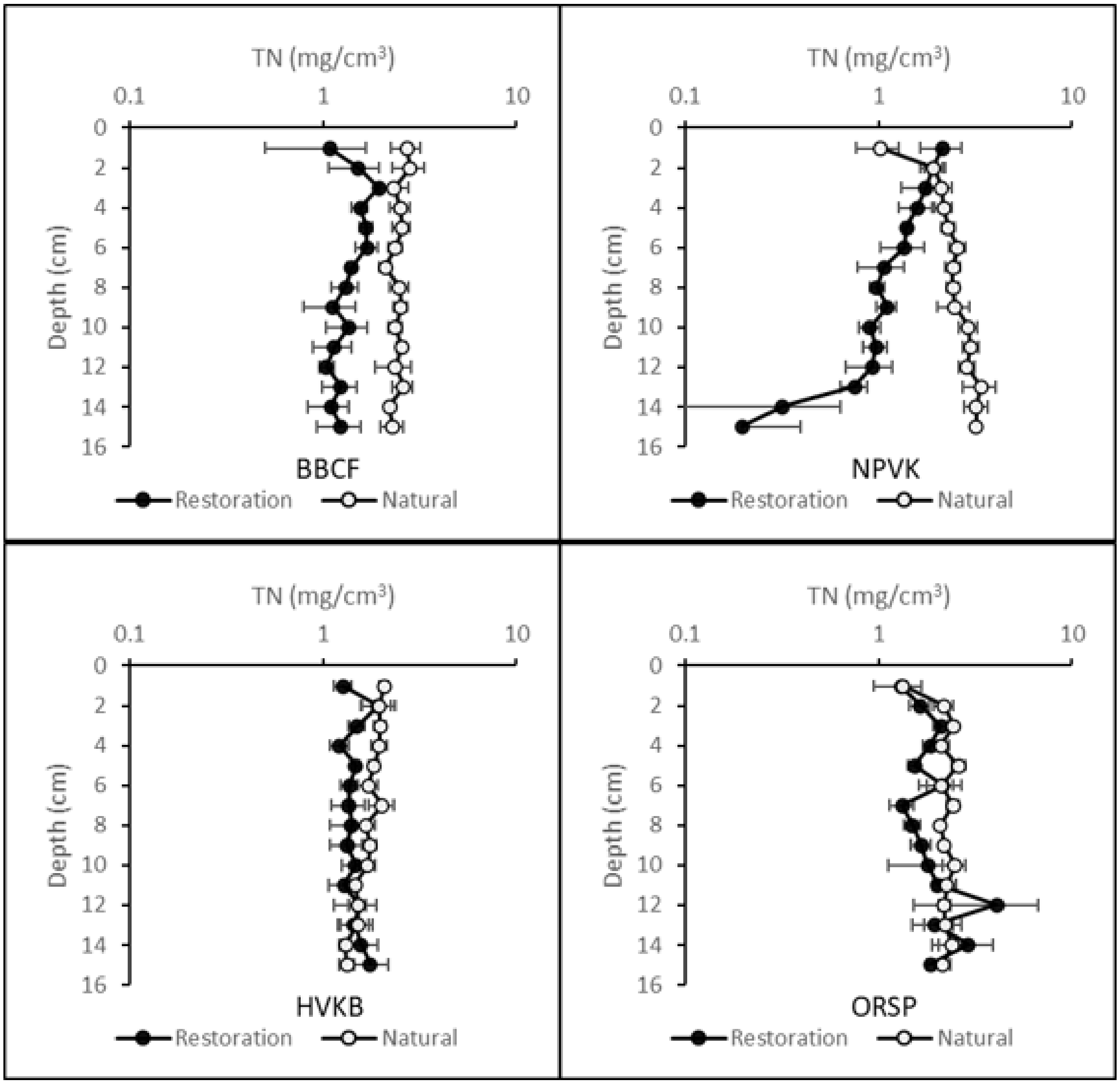

Figure 14: Soil Total Nitrogen over Depth. Soil total nitrogen (TN) content (mg/cm^3) over depth (cm) for restored and natural cores at all four study sites. All values are mean ± SE.

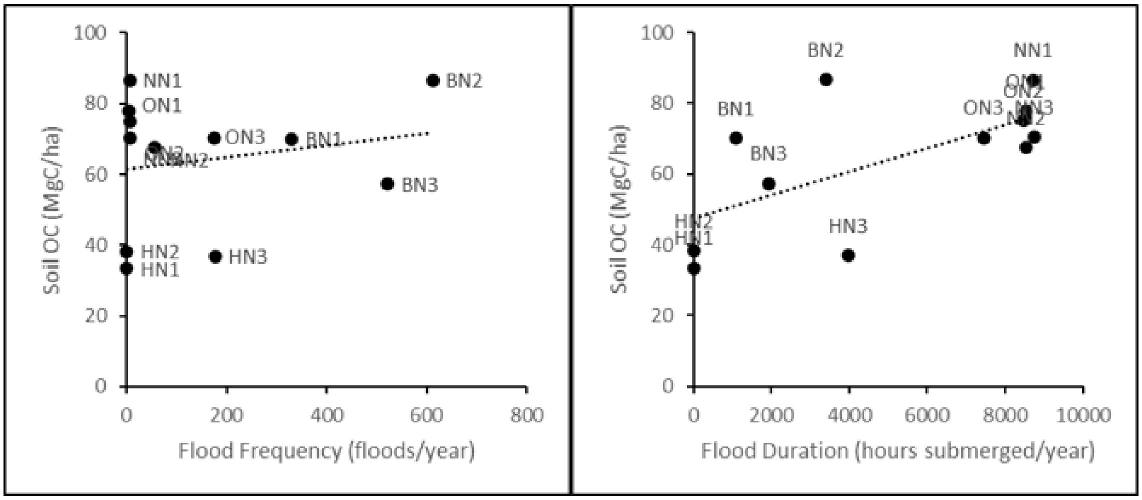

Figure 15: Regression of Soil OC Values at Natural Sites over Hydrology Measures. No linear relationship was found between flood frequency and soil OC in the natural sites (left; r^2 *= 0.039,* $p > 0.05$*). A significant linear relationship of moderate magnitude was found between flood duration and soil OC in the natural sites (right;* r^2 *= 0.423,* $p < 0.05$*).*

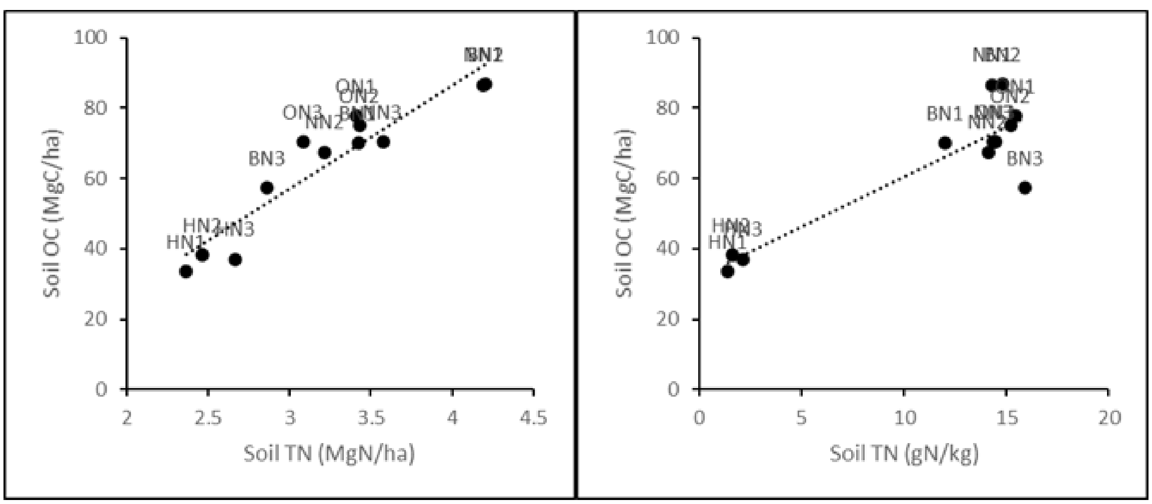

Figure 16: Regression of Soil OC Values at Natural Sites over Soil TN. Soil OC and soil TN had a strong linear relationship across both soil TN by area (left; r^2 *= 0.879,* $p < 0.05$*) and by mass (right;* r^2 *= 0.788,* $p < 0.05$*).*

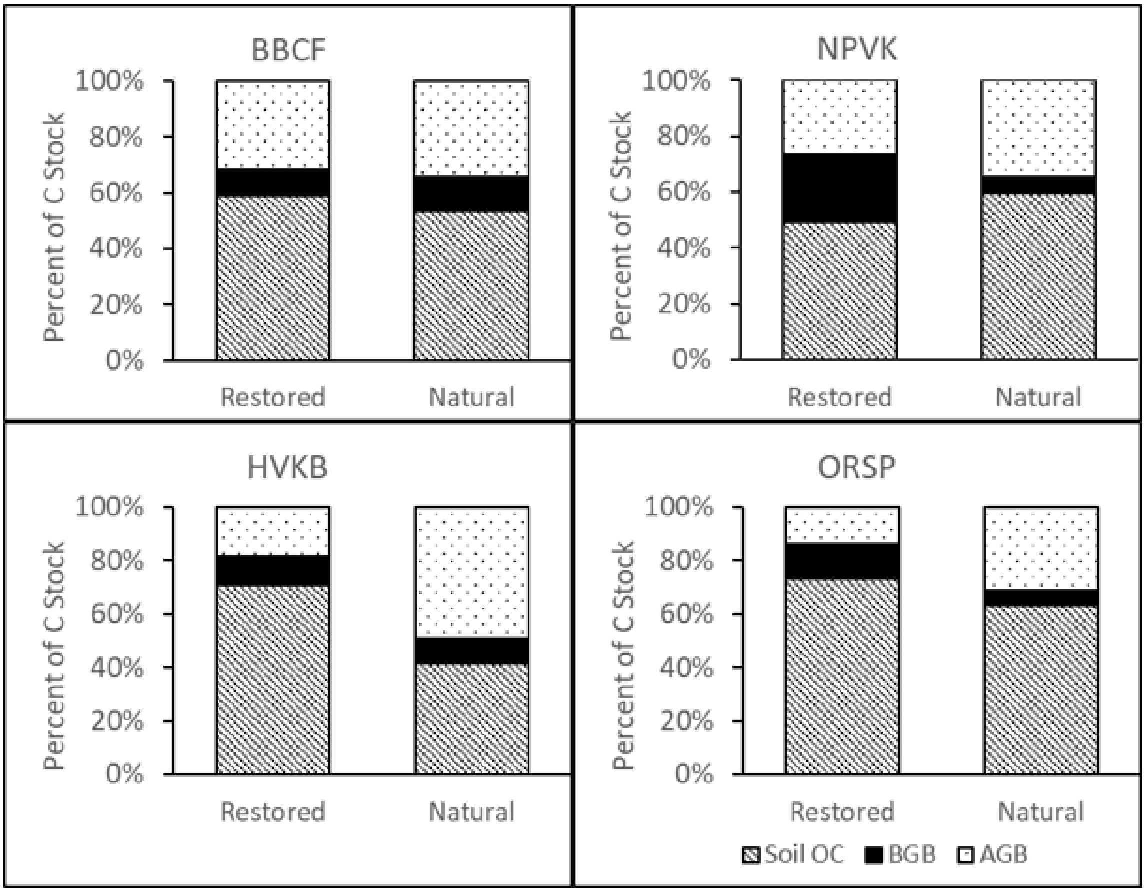

Figure 17: Relative Contribution of Each Carbon Pool to Stock. Percent of C stock provided by soil organic carbon (Soil OC), belowground biomass (BGB), and aboveground biomass (AGB). Data are presented as percent of the mean C stock for each site and management type.

H. Carbon Stock

The total C stock, the sum of all three C pools, ranged from 27.91 to 104.19 MgC/ha (65.50 ± 6.55) in restoration sites, and from 71.73 to 149.41 MgC/ha (116.05 ± 6.41) in natural sites (Table 5). One-way ANOVA found a significant difference in mean C stock among the natural sites [$F(3,8) = 5.966$, $p < 0.05$]. Tukey's post hoc test identified two subgroups, one with HVKB_NAT and one with BBCF_NAT and NPVK_NAT; ORSP_NAT was present in both subgroups. Of the restored-natural pairs, only two sites were significantly different: BBCF [$t(2) = 6.275$, $p < 0.05$] and NPVK [$t(2) = 20.947$, $p < 0.05$].

The mean reference value was 116.05 MgC/ha. C stock over time since restoration showed no linear relationship ($r^2 = 0.041$, $p > 0.05$). The C stock does not display a trend over time, therefore a t_{eq} cannot be calculated from the data collected. Soil OC was the largest C pool for every site-management type pair except HVKB_NAT (Figure 17).

Linear regression analysis was completed to evaluate the relationship between soil C stock and hydrology and soil TN for the four natural sites. There was no significant relationship between C stock and flood frequency or flood duration ($r^2 = 0.173$, $p > 0.05$ and $r^2 = 0.067$, $p > 0.05$, respectively). Soil C stock had a significant positive relationship with both soil TN in Mg/ha ($r^2 = 0.568$, $p < 0.05$) and soil TN in g/kg ($r^2 = 0.533$, $p < 0.05$).

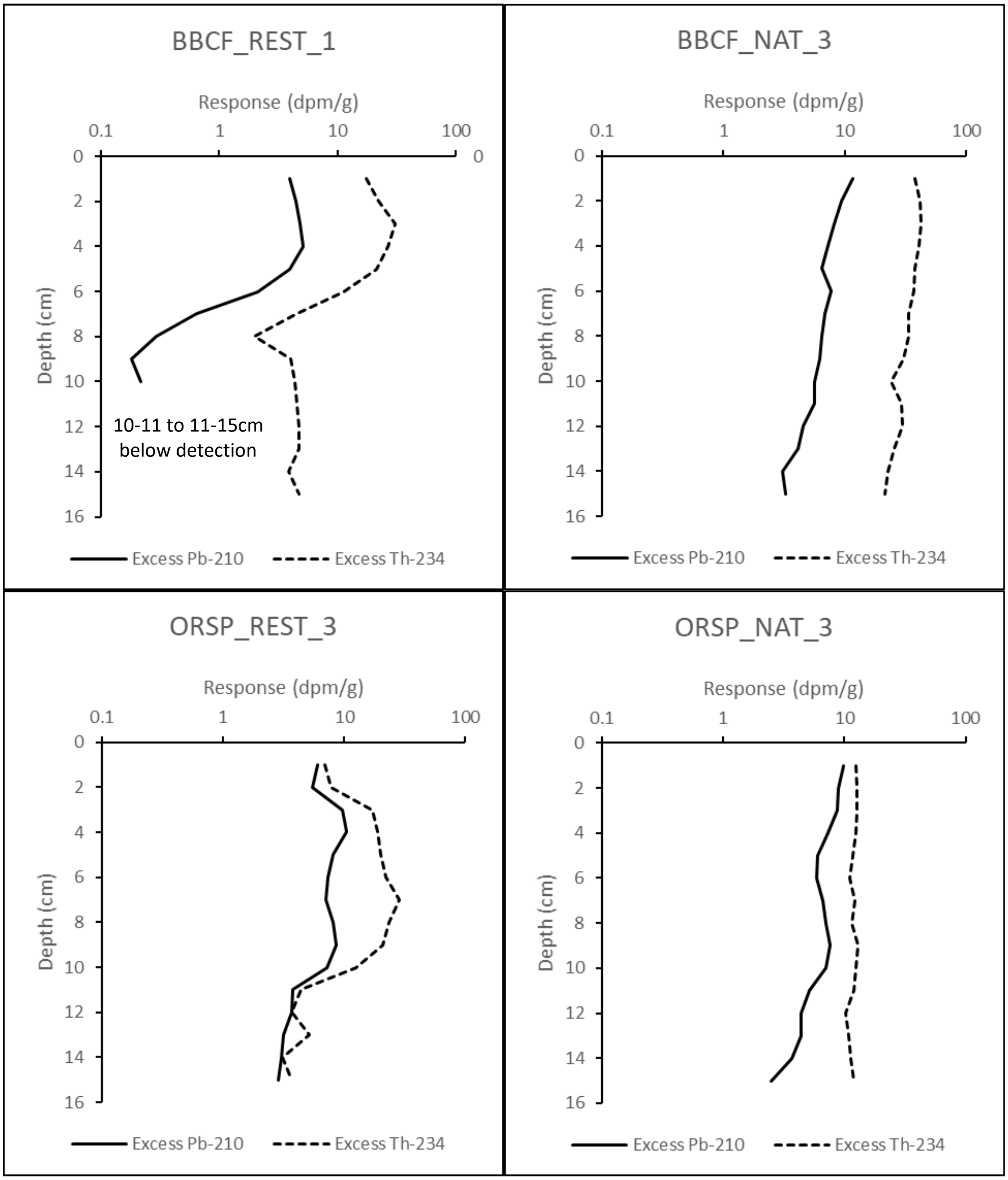

Figure 18: Excess ^{210}Pb and ^{234}Th Activity over Depth. For soil cores from two natural and two restored sites. The natural sites show a steady decline in activity, indicating a steady, relatively uninterrupted accumulation of sediment. The restored sites feature interruptions which may indicate disturbance from the initial restoration or other factors.

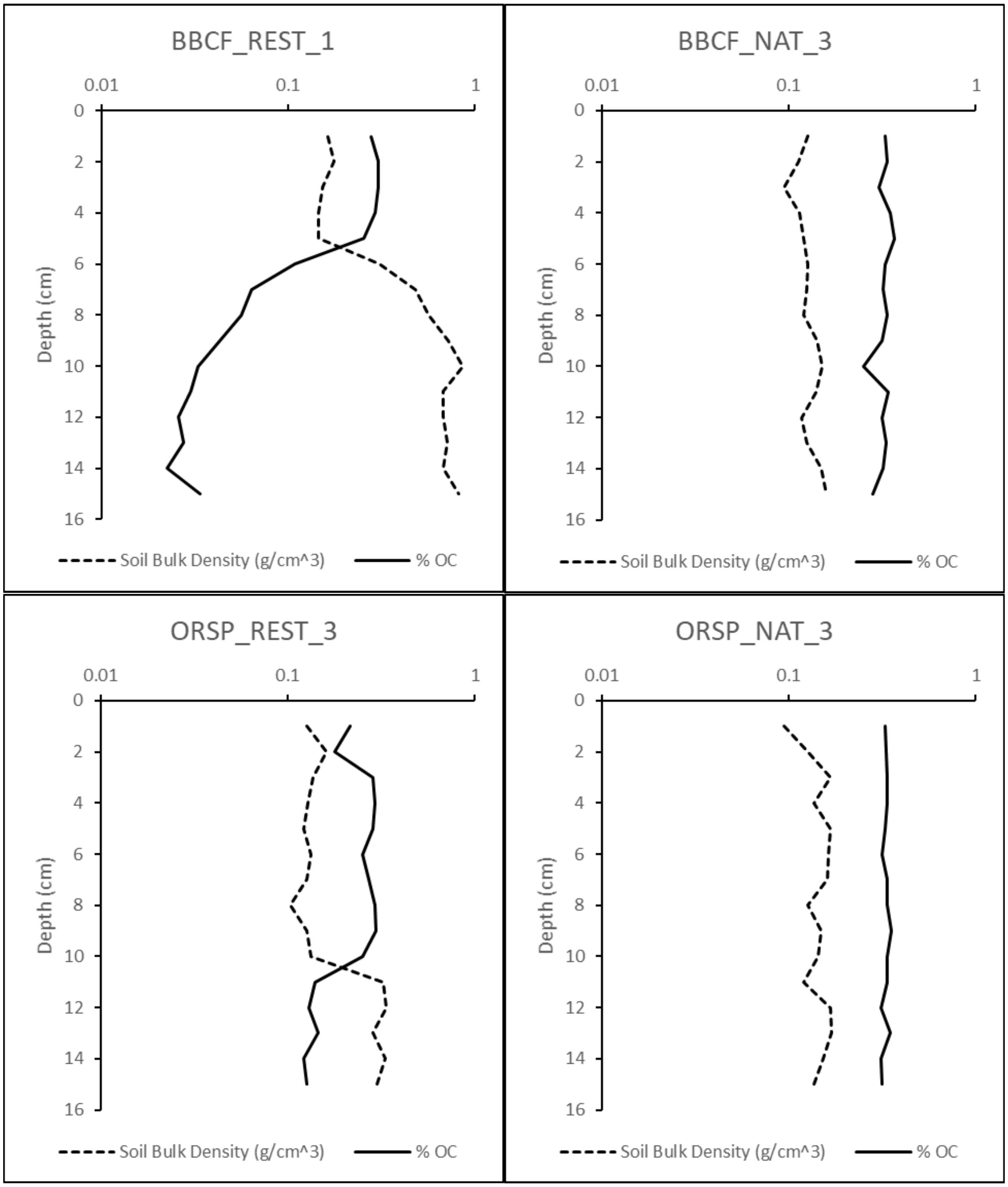

Figure 19: Soil OC % and Bulk Density over Depth. Soil OC % in decimal notation (0.35 = 35% soil OC). For soil cores from two natural and two restored sites. The natural sites maintain relatively stable values of both measurements across their profiles, indicating a steady, relatively uninterrupted accumulation of sediment. The restored sites demonstrate two states, indicating a transition from organic, low-density soils to inorganic, high-density soils.

Table 6: Rates of Sediment Accretion, Mass Accumulation, and Soil OC Accumulation. Rate of sediment accumulation (mm/yr), mass accumulation (g/m^2/yr), and soil OC accumulation (gC/m^2/yr) for one plot at the oldest (BBCF) and youngest (ORSP) restoration sites, and one plot from each of their natural reference sites.

Site	Sediment Accretion Rate (mm/year)	Mass Accumulation Rate (g/m^2/year)	OC Accumulation Rate (gC/m^2/year)
BBCF_REST_1	3.0	521.734	123.789
BBCF_NAT_3	3.9	507.061	161.806
ORSP_REST_3	13.75	1569.596	457.859
ORSP_NAT_3	4.3	638.251	242.025

I. Soil Carbon Accumulation Rate

Excess ^{210}Pb and Th-234 in disintegrations per minute per gram (dpm/g) for the four plots tested for C accumulation rate (BBCF_REST_1, BBCF_NAT_3, ORSP_REST_3, and ORSP_NAT_3) and plotted on a logarithmic scale showed patterns that suggest information about the age of each 1-cm segment (Figure 18). The higher the excess ^{210}Pb in dpm/g, the more recently that layer accumulated. The restoration plot at Bill Baggs Cape Florida (BBCF_REST_1) showed a significant drop-off in excess ^{210}Pb activity after 5-6 cm. The segment at 5-6 cm was therefore interpreted to represent the depth of new sediment accumulated at the site, with lower depths representing either fill material or pre-fill sediment. BBCF_REST_1 also showed a dramatic drop below detection after the 9-10 cm increment. The BBCF restoration was completed 20 years before the sample was taken; considering the results in Figure 18 that 6 cm of sediment accumulated since restoration, the sediment accumulation rate was 3 mm/year. The soil bulk density in this profile ranged from 0.146 g/cm^3 to 0.862 g/cm^3, and the soil OC % ranged from 2.3% to 30.5% (Figure 19). The mass accumulation rate was 521.7 g/m^2/yr, and the soil OC accumulation rate was 123.8 g OC/m^2/yr (Table 6). The natural reference, (BBCF_NAT_3) had a sediment accumulation rate of 3.9 mm/yr, mass accumulation rate of 507.1 g/m^2/yr, and soil OC accumulation rate of 161.8 g C/m^2/yr.

The excess ^{210}Pb profile of the restoration plot at Oleta River State Park (ORSP_REST_3) showed three distinct segments, with a slight drop in activity over the 0-1 cm and 1-2 cm segments, then a relatively steady segment, until a drop-off at the 10-11 cm increment. These three phases make determination of the breaking point between pre-restoration and post-restoration sediment difficult, as either the high or the low point could represent the boundary between new and old sediment. The crossing point between the soil % OC and soil bulk density occurred at the lower drop-off at 10-11 cm, so the deeper point, at the 10-11cm increment, was selected to represent the beginning of the newly accumulated sediment. The ORSP restoration was completed 8 years before the sample was taken; interpreting the results from Figure 18 and Figure 19 to show 11 cm of sediment accumulated since restoration, the sediment accumulation rate was 13.75 mm/yr (a high value but not unheard-of; see Sasmito et al. 2016). The soil bulk density in the profile ranged from 0.103 g/cm^3 to 0.336 g/cm^3, and the soil % OC ranged from 12.2% to 29.4%. The mass accumulation rate was 1,569.6 g/m^2/yr, and the soil OC accumulation rate was 457.9 g C/m^2/yr. The natural reference (ORSP_NAT_3) had a sediment accumulation rate of 4.3 mm/yr, a mass accumulation rate of 638.3 g/m^2/yr, and a soil OC accumulation rate of 242.0 g C/m^2/yr.

Using the sediment accumulation rates and OC accumulation rates from Table 6, the anticipated accumulated OC from an entire 15 cm core of new soil was calculated for each of the cores (Table 7). The predicted soil OC values in BBCF_NAT_3 and

ORSP_REST_3 are very similar to the total soil OC observed in the collected 15 cm soil cores. In contrast, the predicted soil OC in BBCF_REST_1 and ORSP_NAT_3 is slightly higher than the values observed. It is beyond the scope of the present study to explain the discrepancy observed, but future work is recommended to identify potential sources of variation between the predicted and observed soil OC.

Site	Predicted Soil OC in MgC/ha to 15 cm	Observed Soil OC in MgC/ha to 15 cm
BBCF_REST_1	61.5	45.5
BBCF_NAT_3	61.9	57.7
ORSP_REST_3	49.9	50.3
ORSP_NAT_3	84.4	70.3

4. Discussion

A. Carbon Stock and Carbon Pools

This study predicted restored mangrove forests would reach equivalent forest structure and C storage across all three C pools within 20 years. Ultimately, only stem density and C in belowground biomass were found to reach the natural reference value with a t_{eq} < 20 years, with values for other measurements ranging from 29.2 years for average mangrove height to 62.2 years for basal area. Soil OC did not trend toward the natural reference value, so t_{eq} could not be calculated. Because soil OC made up the largest component of the C stock across all sites and management types (except HVKB_NAT), the trend in C stock was weakened below significance, so t_{eq} could not be calculated for C stock either.

Early growth mangrove restorations in South Florida were previously studied by Osland et al. (2012) in the mangroves around Tampa Bay. Osland et al. studied 9 natural and 9 restored mangrove forests in the Tampa Bay area, representing a 20-year chronosequence. Their study examined soil cores in two groupings, the soils from the top 10 cm from the surface (0 – 10 cm) and the soils from 10 to 30 cm deep. Soil organic matter (in %), TN (in g/kg), and soil TC (in g/kg) in the top 10 cm of soil were found to reach equivalence in approximately 20 years. Soil bulk density and soil moisture percent in the top 10 cm were predicted to reach equivalence in 30 years. The 10-30 cm soil core segments did not trend toward equivalence in any of sites studied by Osland et al. The t_{eq} for aboveground biomass in the present study (50.4 years) was considerably higher than that found by Osland et al. Using a nonlinear regression model, Osland et al. predicted a t_{eq} of 25 years for mean adult tree diameter (Osland et al. 2012). Osland et al.'s study analyzed adult and juvenile mangrove trends separately, classifying trees with DBH > 6 cm as "adult mangroves." The adult mangrove tree diameter was selected for comparison to the present study as diameter was the measurement used in the allometric equation for aboveground biomass; comparison to average DBH, however, was very similar (t_{eq} = 47 years).

The comparison to Osland et al. (2012) highlights one of the challenges in studying restored ecosystems, which is that there is not one standard method or unit used for studying restored forests. As mentioned above, Osland et al. (2012) measured the trees above 6 cm DBH as "adult trees," but in the present study, two of the four restoration sites did not contain a single mangrove with a DBH greater than or equal to 6 cm. The results are therefore highly sensitive to the criteria for inclusion, and the methods used in mature forests may not be suitable to conditions in a restored forest. Pool et al.

(1977) and Castañeda-Moya et al. (2013) measured DBH of all trees over 2.5 cm. Other studies measure all trees in a plot with DBH over 5 cm (Friess et al. 2016), sometimes going on to account for trees thinner than 5 cm by subsampling their vegetation plots (Howard et al. 2014). Studies can be compared through conversion to common units, but the fundamental resolutions will vary according to how each study defines and accounts for seedlings, saplings, and small trees. In the present study, in order to capture the smaller mangroves common in recent restorations, Pool et al. (1977) were followed in using the 2.5 cm threshold for inclusion, with everything smaller than 2.5 cm DBH excluded.

As with aboveground biomass, belowground biomass measurements are sensitive to the chosen collection method. Sampling root biomass through soil cores is inherently subject to a bias excluding large roots that resist the cutting strength of the corer, as well as sampling bias that prioritizes a flat soil surface for collecting a solid soil core (Adame et al. 2017). Species-specific allometric equations for belowground biomass are less commonly calculated than species-specific equations for aboveground biomass due to the highly destructive and labor-intensive process of excavating the full root system of a mangrove (Howard et al. 2014). Komiyama (2005) produced a general equation for belowground biomass in mangroves as a function of wood density and DBH. Adame et al. (2017) found the general equation produced biomass values 40 ± 12% larger than values derived from field measurements; however, they note it is not clear whether this difference is due to overestimation of biomass by the allometric equations or underestimation of biomass by the field measurements. As the present study required the removal of roots from soil cores, the directly sampled values were selected for study rather than making use of the general equation. Because the central question of the present study is comparative in nature, the uncertainty introduced by choosing one method over the other should not affect my conclusions for belowground biomass; however, the observed belowground biomass may be lower than the true value. Similarly, the soil OC in the present study accounts for only the top 15 cm of soil, as the restorations were anticipated not to have accumulated more than 15 cm, so the total C stock reported here cannot be directly compared with total stock in sites using cores 30 cm deep, 1 m deep, or deeper. A close comparison would be Dontis et al. (2020), who found a soil OC stock of 24.3 ± 4.3 MgC/ha in the top 10 cm of mangroves forests between 14 and 26 years of age; the top 10 cm of soil in the oldest site in the present study (BBCF) contained slightly more C at 29.9 MgC/ha.

To understand why soil OC in the restored sites did not trend to equivalence with the natural sites, the influence of environmental factors such as hydrology and TN content must be considered. Previous research on mangroves in South Florida has focused on the natural mangrove forests in Taylor Slough and Shark River Slough in the Florida Everglades (Castañeda-Moya et al. 2013). From 2001 to 2005, Taylor Slough had flood frequencies ranging across sites from 6 to 48 floods per year, with flood durations ranging from 3,541 to 8,653 hours per year. In the same time period, Shark River Slough sites experienced 165 to 395 floods per year and 3,965 to 5,592 hours per year of flooding. The restored sites in the present study had flood duration values within the range of values seen at Taylor Slough and exceeding the flood duration values at Shark

River Slough; thus it seems the hydrology of the restored sites are within a range that can support natural mangrove forest growth. The natural reference sites in the present study present a more complicated picture, with the natural sites at HVKB and BBCF flooding for approximately one fourth of the total annual flood duration of the other natural and restored sites in this study. This difference in hydrology suggests that incorporating hydrology directly into the site selection process would influence the C storage results. The linear regression of soil OC versus flood duration showed a positive relationship of moderate explanatory power (Figure 15); however, excluding HVKB_NAT with its significantly lower soil OC and overall low flood duration (with two plots never submerged over the course of the study) eliminates this relationship: looking at only the remaining 9 natural plots, there is no significant relationship between soil OC and flood duration ($r^2 = 0.085$, $p = 0.445$). Accordingly, hydrology does not seem to be a primary driver of soil OC in these sites, and the explanation for the failure of restored soil OC to trend to equivalence with the natural sites must lie elsewhere.

Soil TN is another environmental factor that could be driving deviation in soil OC. Soil TN and soil OC were shown to have a strong, significant relationship, as documented in Figure 16; however, this relationship cannot speak to causality. A major source of N in mangrove soils is the *in-situ* decomposition of organic material; the relationship between soil OC and TN may be due to their sharing a common source. Previous research proposed treating soil TN as an indicator of mangrove restoration success rather than an environmental factor contributing to that success (Salmo et al. 2013).

It is possible the relationship between the soil OC in the sites is being obscured by another factor not measured in the present study. For example, phosphorus (P) is known to increase soil OC in mangroves (Rovai et al. 2018); analysis of soil P or aquatic inputs of N or P may explain the observed soil OC. The sites may also differ in their exposure to storm sediment and nutrient inputs, a significant fertilization source for mangroves elsewhere in South Florida (Castañeda-Moya et al. 2020).

Similar to the present study, Dontis et al. (2020) also found no relationship between soil OC stock and site age in mangrove forests up to 26 years in age. In their study, Dontis et al. suggested this could be a function of soil C accumulating more slowly than aboveground C, predicting that with more time the relationship would become evident (Dontis et al. 2020). Accordingly, revisiting the present study sites in the future may enable a lagging trend to become evident.

B. Soil Carbon Accumulation Rate

Because of the resource-intensive nature of the ^{210}Pb process, only four cores were able to be analyzed for this study. Selected for study were one core each from the oldest (BBCF) and youngest (ORSP) restoration sites (20 and 8 years old, respectively, at time of sampling), as well as one core from their respective reference sites. Soil OC accumulation in the restored mangroves of the present study was estimated at 123.79 g OC/m^2/yr at BBCF_REST_1 and 457.86 g/m^2/yr at ORSP_REST_3, while soil OC accumulation in the natural mangroves was estimated at 161.81 g/m^2/yr at BBCF NAT 3 and 242.03 g/m^2/yr at ORSP NAT 3. Previous studies of soil OC accumulation vary considerably. Breithaupt et al. (2012) conducted a meta-analysis of 19 primary research studies evaluating use of ^{210}Pb and ^{137}Cs in natural mangrove soils around the world to determine soil accumulation rate (SAR) and OC burial rate (Breithaupt et al. 2012). They found a global average OC burial rate of 163 g/m^2/yr over 100 years (geometric mean; 95% CI from 131.3 to 202.5), which was an intermediate value compared to 7 previously determined global values from other studies ranging from 100 – 226 g/m^2/yr. An approximately contemporary estimate from Alongi (2012) reported a global mangrove OC burial rate of 174 g C/m^2/yr.

Looking at restored mangrove forests specifically, Lunstrum and Chen (2014) studied two young mangrove forests in the Futian National Natural Reserve in Shenzen, Guangdong, China. These two forests, consisting of a mix of mangrove species *Kandela obovata* and *Sonneratia apetala*, were studied every year for 6 years after the completion of restoration, and were found to accumulate C at a rate of 155 gC/m^2/yr, which they compared to similar studies with 139 and 255 gC/m^2/yr. Within South Florida, Osland et al. (2012) found a C storage rate in a South Florida mangrove restoration of 218 gC/m^2/yr.

In the present study, sediment accretion in the restored sites was 3 mm/yr at BBCF_REST_1 and 13.75 mm/yr at ORSP_REST_3, while in the natural sites sediment accretion was 3.9 mm/yr at BBCF_NAT_3 and 4.3 mm/yr at ORSP_NAT_3. Sediment accretion varies widely between sites and between studies. Breithaupt et al.'s (2012) meta-analysis reported a median global mangrove SAR of 2.8 mm/yr (95% CI: 1.9 to 3.9). Sasmito et al. (2016) conducted a meta-analysis of SAR in mangrove forests; for forests in Florida, SAR ranged from 1 (SD not reported) to 11.5 ± 11.7 mm/yr (standard deviation), not including an outlier of 77 mm/yr observed following a major storm event (Sasmito et al. 2016). When grouped by site condition, the studies of pristine mangrove forests had SAR of 5.49 ± 0.49, while restored mangroves had an SAR of 4.82 ± 1.16 mm/yr.

Krauss et al. (2017) compared the overall surface elevation change (the net change in surface elevation from all factors, including SAR, root expansion, and soil subsidence) to the rate of sea-level rise (SLR; Krauss et al. 2017). Reporting a rate of relative SLR in Tampa Bay of 2.6 mm/yr, Krauss et al. (2017) found restored mangroves (aged 7.1 to 25.1 years) to consistently outpace SLR with vertical surface elevation change rates of 4.2 mm/yr to 11 mm/yr. The natural sites in Krauss et al. (2017) were more complicated, with some sites having surface elevation change as low as 1.5 mm/yr (below the rate of relative SLR) and others as high as 7.2 mm/yr. The contribution to surface elevation change from SAR in Krauss et al. (2017) ranged from 3.7 mm/yr to 9.1 mm/yr across both treatments. The difference observed between the natural and restored sites was explained by the high root growth found in young mangroves. The authors noted that as the restored mangroves become more established, the subsurface vertical gains will decrease as some of the roots begin decomposing and the soils compress. The present study did not account directly for subsurface change or changes in C storage over the life cycle of the mangrove restorations; similar subsurface vertical gains from root growth could explain the extremely high vertical growth observed at the ORSP_REST site. If rapid growth in a young restoration explains the vertical gains recorded as the

ORSP_REST sediment accretion rate, the rate will slow as the restoration ages. To evaluate how the rates of sediment accumulation and C storage change over time, further study of the subject restorations is recommended as the restorations age.

Breithaupt et al. (2014) noted that the time frame of measurement is significant when estimating both soil C accumulation rate and SAR, with C storage estimates over a short period time being more likely to overestimate C storage potential (Breithaupt et al. 2014). In their study of South Florida mangroves along the Shark River in Everglades National Park, soil OC over a 10 year period was estimated at 225 ± 60 $gC/m^2/yr$, whereas soil OC over a 50 and 100-year period gave estimates of 176 ± 31 and 123 ± 19 $gC/m^2/yr$, respectively. Similarly, in the same study, SAR was estimated at 4.8 ± 1.0 mm/yr over a 10-year period, 3.7 ± 0.7 mm/yr over a 50-year period, and 2.7 ± 0.4 over a 100-year period. However, a more recent exploration of the distinction between recent and long-term rates has proposed the increased rates over shorter timeframes may represent a true increase in accumulation rates, perhaps driven by sea level rise (Breithaupt et al. 2020). Further study will be needed to determine whether the rates observed in the present study decrease with time or if they represent a response to rising sea levels.

C. Carbon Capture and Loss

The discussion above has implicitly considered each study site as a closed system, capturing C on-site that is then entirely conserved; however, mangrove ecosystems are known to both retain C captured elsewhere (allochthonous C) and to export C captured on-site (autochthonous C) out of the ecosystem. Allochthonous C has been shown to have a relatively short residence time in mangroves, with mangrove roots making up significantly more of the soil C retained at depth (Saintilan et al 2013). The present study did not distinguish between allochthonous and autochthonous C, so allochthonous inputs remain a potential source of variation within the sites.

Just as much of the allochthonous C that passes through mangrove ecosystems is eventually flushed out of the system, a significant portion of the organic matter produced on-site (autochthonous C) is exported rather than retained (Ribeiro et al. 2019). Change in C or N after deposition is referred to as “diagenesis,” and can include physical loss of soil or organic matter and chemical loss through microbial processes (Brahney et al. 2014). Within blue carbon ecosystems like mangrove forests, saturation from tidal submersion dramatically decreases the available oxygen, creating an anoxic environment that slows oxidation and conserves buried soil C (Howard et al. 2014). However, infrequent tidal flushing can expose mangrove soils to oxygen, allowing oxidation of the buried plant matter, breaking up C that is subsequently lost to the air or water. Some restored mangrove forests have been observed to produce nitrous oxide and methane in the presence of untreated wastewater (Konnerup et al. 2014). Incorporation of aquatic nutrients and atmospheric C flux into future study can provide insight into the total C balance in the restored mangrove forests in Biscayne Bay.

D. Disturbance by Storms

Another area for future study is the role of disturbance by storm events in both the restorations and natural forests. Tropical storms are recurring disturbance events in mangrove forests, causing forest defoliation and downed trees (Alongi 2008). Morphological traits like wide, branching root systems enable mangroves to resist wind and wave energy from storms (McIvor et al. 2012). Regular occurrence of tropical storm events can, along with precipitation and temperature, is a control on the local maximum height observed in mangrove forests (Simard et al. 2019). In South Florida, mangroves in the Florida Coastal Everglades suffered low mortality from a Category 3 hurricane and recovered from defoliation by the storm in approximately 10 years (Rivera-Monroy et al. 2019). Deposition of high-phosphorus marine sediment has been shown to naturally facilitate rapid post-storm recovery in the Florida Everglades (Castañeda-Moya et al. 2020), but storm events on stressed mangroves can result in catastrophic losses to the forest as a whole (Lewis et al. 2016).

Hurricane Irma struck South Florida, USA, during the course of data collection for the present study, after collecting all aboveground vegetation measurements but prior to initiating hydrological data collection or collecting soil cores. Hurricane Irma did not hit Biscayne Bay directly, hitting Florida farther south in the Florida Keys (Radabaugh et al. 2020). None of the tagged mangrove trees in any plot were downed by Hurricane Irma; however, following Hurricane Irma, the restoration at the Historic Virginia Key Beach Park suffered high mortality, possibly due to storm-related interruption of the tidal channel, which may explain the distinctively constrained hydrograph observed in Figure 3.

5. Conclusion

The present study sought to quantify the C storage trajectory of early growth mangrove restorations in Miami-Dade County, Florida, USA. The study did not show a linear relationship between C stock and time since restoration; however, the summed values in the C stock measurement mask individual trends by C pool. The C in aboveground biomass was approaching equivalence, with a t_{eq} = 50.4 years. The belowground root biomass C had already reached equivalence by the 20-year mark, with a t_{eq} of 13.6 years. The soil OC did not display a trend over time. Additional study sites may have enabled a more complex, non-linear pattern to be discerned. Alternately, revisiting the existing sites in the future could enrich this snapshot of the C storage potential of these restorations. By continuing to study and refine our understanding of the C storage potential of mangrove forests, the scale of benefit to be achieved by existing restorations can be determined, and the scale of action needed to fully mitigate the change in our climate can be defined.

6. List of References

Adame, M. F., S. Cherian, R. Reef, and B. Stewart-Koster. 2017. Mangrove root biomass and the uncertainty of belowground carbon estimations. Forest Ecology and Management 403:52–60.

Alongi, D. M. 2008. Mangrove forests: Resilience, protection from tsunamis, and responses to global climate change. Estuarine, Coastal and Shelf Science 76:1–13.

Alongi, D. M. 2012. Carbon sequestration in mangrove forests. Carbon Management 3:313–322.

Alongi, D. M. 2014. Carbon cycling and storage in mangrove forests. Annual Review of Marine Science 6:195–219.

Brahney, J., A. P. Ballantyne, B. L. Turner, S. A. Spaulding, M. Otu, and J. C. Neff. 2014. Separating the influences of diagenesis, productivity and anthropogenic nitrogen deposition on sedimentary δ15N variations. Organic Geochemistry 75:140–150.

Breithaupt, J. L., J. M. Smoak, T. S. Bianchi, D. R. Vaughn, C. J. Sanders, K. R. Radabaugh, M. J. Osland, L. C. Feher, J. C. Lynch, D. R. Cahoon, G. H. Anderson, K. R. T. Whelan, B. E. Rosenheim, R. P. Moyer, and L. G. Chambers. 2020. Increasing Rates of Carbon Burial in Southwest Florida Coastal Wetlands. Journal of Geophysical Research: Biogeosciences 125:1–25.

Breithaupt, J. L., J. M. Smoak, T. J. Smith, and C. J. Sanders. 2014. Temporal variability of carbon and nutrient burial, sediment accretion, and mass accumulation over the past century in a carbonate platform mangrove forest of the Florida Everglades. Journal of Geophysical Research G: Biogeosciences 119:2032–2048.

Breithaupt, J. L., J. M. Smoak, T. J. Smith, C. J. Sanders, and A. Hoare. 2012. Organic carbon burial rates in mangrove sediments: Strengthening the global budget. Global Biogeochemical Cycles 26:1–11.

Castañeda-Moya, E., V. H. Rivera-Monroy, R. M. Chambers, X. Zhao, L. Lamb-Wotton, A. Gorsky, E. E. Gaiser, T. G. Troxler, J. S. Kominoski, and M. Hiatt. 2020. Hurricanes fertilize mangrove forests in the Gulf of Mexico (Florida Everglades, USA). Proceedings of the National Academy of Sciences of the United States of America 117:4831–4841.

Castañeda-Moya, E., R. R. Twilley, and V. H. Rivera-Monroy. 2013. Allocation of biomass and net primary productivity of mangrove forests along environmental gradients in the Florida Coastal Everglades, USA. Forest Ecology and Management 307:226–241.

Crooks, S., L. Windham-Myers, and T. G. Troxler. 2019. Defining Blue Carbon. Pages 1–8 *in* L. Windham-Myers, S. Crooks, and T. G. Troxler, editors. A Blue Carbon Primer: The State of Coastal Wetland Carbon Science, Practice, and Policy. CRC Press, Boca Raton, FL.

Das, S., and A. S. Crépin. 2013. Mangroves can provide protection against wind damage during storms. Estuarine, Coastal and Shelf Science 134:98–107.

Donato, D. C., J. B. Kauffman, D. Murdiyarso, S. Kurnianto, M. Stidham, and M. Kanninen. 2011. Mangroves among the most carbon-rich forests in the tropics. Nature Geoscience 4:293–297.

Dontis, E. E., K. R. Radabaugh, A. R. Chappel, C. E. Russo, and R. P. Moyer. 2020. Carbon Storage Increases with Site Age as Created Salt Marshes Transition to Mangrove Forests in Tampa Bay, Florida (USA). Estuaries and Coasts 43:1470–1488.

Emmer, I. M., B. A. Needelman, S. Emmett-Mattox, S. Crooks, J. P. Megonigal, D. Myers, M. P. J. Oreska, K. J. McGlathery, D. Shoch, V. C. S. Methodology, and S. Scope. 2015. Methodology for Tidal Wetland and Seagrass Restoration:1–115.

Ewe, S. M. L., E. E. Gaiser, D. L. Childers, D. Iwaniec, V. H. Rivera-Monroy, and R. R. Twilley. 2006. Spatial and temporal patterns of aboveground net primary productivity (ANPP) along two freshwater-estuarine transects in the Florida Coastal Everglades. Hydrobiologia 569:459–474.

Feller, I. C., C. E. Lovelock, U. Berger, K. L. McKee, S. B. Joye, and M. C. Ball. 2010. Biocomplexity in mangrove ecosystems. Annual review of marine science 2:395–417.

Florida Department of Environmental Protection. 2008. Oleta River State Park Unit Management Plan.

Folke, C., S. Carpenter, B. Walker, M. Scheffer, T. Elmqvist, L. Gunderson, and C. S. Holling. 2004. Regime Shifts, Resilience, and Biodiversity in Ecosystem Management. Annual Review of Ecology, Evolution, and Systematics 35:557–581.

Friess, D. A., D. R. Richards, and V. X. H. Phang. 2016. Mangrove forests store high densities of carbon across the tropical urban landscape of Singapore. Urban Ecosystems 19:795–810.

Harlem, P. 1979. Aerial photographic interpretation of the historical changes in northern Biscayne Bay, Florida, 1925 to 1976. University of Miami.

Howard, J., S. Hoyt, K. Isensee, E. Pidgeon, and M. Telszewski. 2014. Coastal Blue Carbon: Methods for assessing carbon stocks and emissions factors in mangroves, tidal salt marshes, and seagrass meadows. Arlington, Virginia.

Krauss, K. W., N. Cormier, M. J. Osland, M. L. Kirwan, C. L. Stagg, J. A. Nestlerode, M. J. Russell, A. S. From, A. C. Spivak, D. D. Dantin, J. E. Harvey, and A. E. Almario. 2017. Created mangrove wetlands store belowground carbon and surface elevation change enables them to adjust to sea-level rise. Scientific Reports 7:1030.

Lewis, R. R., E. C. Milbrandt, B. Brown, K. W. Krauss, A. S. Rovai, J. W. Beever, and L. L. Flynn. 2016. Stress in mangrove forests: Early detection and preemptive rehabilitation are essential for future successful worldwide mangrove forest management. Marine Pollution Bulletin 109:764–771.

Liddell, K. 2003. Summary Report: Long-Term Monitoring of Restored Coastal Habitats. Miami, FL.

Lovelock, C. E., D. A. Friess, J. B. Kauffman, and J. W. Fourqurean. 2019. Human Impacts on Blue Carbon Ecosystems. Pages 17–24 *in* L. Windham-Myers, S. Crooks, and T. G. Troxler, editors. A Blue Carbon Primer: The State of Coastal Wetland Carbon Science, Practice and Policy. CRC Press, Boca Raton, FL.

McIvor, A., I. Möller, T. Spencer, and M. Spalding. 2012. Reduction of Wind and Swell Waves by Mangroves. Page Natural Coastal Protection Series.

Miami-Dade County. 2010. Greenprint: Climate Change Action Plan.

Milano, G. R. 1999a. Restoration of coastal wetlands in southeastern florida. Wetland Journal 11:15–24.

Milano, G. R. 1999b. Cape Florida State Recreation Area Wetlands Restoration. Proceedings of the Twenty Fifth Annual Conference on Ecosystems Restoration and Creation:110–119.

Milano, G. R. 2000. Island restoration and enhancement in Biscayne Bay, Florida. Proceedings of the 26th Annual Conference on Ecosystem Restoration and Creation:1–17.

Mukherjee, N., W. J. Sutherland, M. N. I. Khan, U. Berger, N. Schmitz, F. Dahdouh-Guebas, and N. Koedam. 2014. Using expert knowledge and modeling to define mangrove composition, functioning, and threats and estimate time frame for recovery. Ecology and Evolution 4:2247–2262.

Nagelkerken, I., S. J. M. Blaber, S. Bouillon, P. Green, M. Haywood, L. G. Kirton, J. O. Meynecke, J. Pawlik, H. M. Penrose, A. Sasekumar, and P. J. Somerfield. 2008. The habitat function of mangroves for terrestrial and marine fauna: A review. Aquatic Botany 89:155–185.

Osland, M. J., A. C. Spivak, J. A. Nestlerode, J. M. Lessmann, A. E. Almario, P. T. Heitmuller, M. J. Russell, K. W. Krauss, F. Alvarez, D. D. Dantin, J. E. Harvey, A. S. From, N. Cormier, and C. L. Stagg. 2012. Ecosystem Development After Mangrove Wetland Creation: Plant-Soil Change Across a 20-Year Chronosequence. Ecosystems 15:848–866.

Radabaugh, K. R., R. P. Moyer, A. R. Chappel, E. E. Dontis, C. E. Russo, K. M. Joyse, M. W. Bownik, A. H. Goeckner, and N. S. Khan. 2020. Mangrove Damage, Delayed Mortality, and Early Recovery Following Hurricane Irma at Two Landfall Sites in Southwest Florida, USA. Estuaries and Coasts 43:1104–1118.

Ribeiro, R. de A., A. S. Rovai, R. R. Twilley, and E. Castañeda-Moya. 2019. Spatial variability of mangrove primary productivity in the neotropics. Ecosphere 10.

Rivera-Monroy, V. H., T. M. Danielson, E. Castañeda-Moya, B. D. Marx, R. Travieso, X. Zhao, E. E. Gaiser, and L. M. Farfan. 2019. Long-term demography and stem productivity of Everglades mangrove forests (Florida, USA): Resistance to hurricane disturbance. Forest Ecology and Management 440:79–91.

Romañach, S. S., D. L. DeAngelis, H. L. Koh, Y. Li, S. Y. Teh, R. S. Raja Barizan, and L. Zhai. 2018. Conservation and restoration of mangroves: Global status, perspectives, and prognosis. Ocean and Coastal Management 154:72–82.

Rovai, A. S., R. R. Twilley, E. Castañeda-Moya, P. Riul, M. Cifuentes-Jara, M. Manrow-Villalobos, P. A. Horta, J. C. Simonassi, A. L. Fonseca, and P. R. Pagliosa. 2018. Global controls on carbon storage in mangrove soils. Nature Climate Change 8:534–538.

Salmo, S. G., C. Lovelock, and N. C. Duke. 2013. Vegetation and soil characteristics as indicators of restoration trajectories in restored mangroves. Hydrobiologia 720:1–18.

Salmo, S. G., C. E. Lovelock, and N. C. Duke. 2014. Assessment of vegetation and soil conditions in restored mangroves interrupted by severe tropical typhoon "Chan-hom" in the Philippines. Hydrobiologia 733:85–102.

Sasmito, S. D., D. Murdiyarso, D. A. Friess, and S. Kurnianto. 2016. Can mangroves keep pace with contemporary sea level rise? A global data review. Wetlands Ecology and Management 24:263–278.

Simard, M., L. Fatoyinbo, C. Smetanka, V. H. Rivera-Monroy, E. Castañeda-Moya, N. Thomas, and T. Van der Stocken. 2019. Mangrove canopy height globally related to precipitation, temperature and cyclone frequency. Nature Geoscience 12:40–45.

Smith, T. J., and K. R. T. Whelan. 2006. Development of allometric relations for three mangrove species in South Florida for use in the Greater Everglades Ecosystem restoration. Wetlands Ecology and Management 14:409–419.

Smoak, J. M., J. L. Breithaupt, T. J. Smith, and C. J. Sanders. 2013. Sediment accretion and organic carbon burial relative to sea-level rise and storm events in two mangrove forests in Everglades National Park. Catena 104:58–66.

Smoak, J. M., and S. R. Patchineelam. 1999. Sediment mixing and accumulation in a mangrove ecosystem: Evidence from 210Pb, 234Th and 7Be. Mangroves and Salt Marshes 3:17–27.

Teas, H. J. 1974. Mangroves of Biscayne Bay. Report to Metropolitan Dade County Commission.

Virginia Key Master Plan. 2010. . Miami, FL. http://archive.miamigov.com/planning/docs/plans/vk/4_virginia_key_final_report.pdf.

Zhang, K., H. Liu, Y. Li, H. Xu, J. Shen, J. Rhome, and T. J. Smith. 2012. The role of mangroves in attenuating storm surges. Estuarine, Coastal and Shelf Science 102–103:11–23.